Universiti Malaysia PAHANG

RESEARCH REPORT UMP GRANT
Laporan Prestasi Skim Geran UMP

Final	√	Progress		*Progress Period :* _____	√ *Please tick*

PROJECT DETAILS *(Keterangan Projek)*

A

Grant No	RDU1503101
Faculty/CoE	FACULTY OF MECHANICAL AND AUTOMOTIVE ENINEERING TECHNOLOGY
Project Title	BIODIESEL-DIESEL (UP TO 45%) FUEL CHARACTERISTICS ON HOMOGENEOUS CHARGE COMPRESSION IGNITION ENGINE
Project Leader	PROF. TS. DR. MD MUSTAFIZUR RAHMAN
Project Member	1. PM DR KUMARAN KADIRGAMA, FTKMA 2. PM DR DEVARAJAN RAMASAMY, FTKMA 3. PM DR WAN SHARUZI WAN HARUM, FTKMA 4. PROF. DR. RIZALMAN BIN MAMAT, FTKMA 5. DR. MUHAMAD MAT NOOR, FTKMA

PROJECT ACHIEVEMENT *(Pencapaian Projek)*

B

ACHIEVEMENT PERCENTAGE				
Project progress according to milestones achieved up to this period	**0 - 25%**	**26 - 50%**	**51 - 75%**	**76 - 100%**
Percentage (please state %)				100%

EXPENDITURE *(Perbelanjaan)*

C

Budget Approved *Peruntukan diluluskan*	**Amount Spent** *Jumlah Perbelanjaan*	**Balance** *Baki*	**% of Amount Spent** *Peratusan Belanja*
RM39,790.00	**RM39,651.60**	**RM138.40**	**99.65 %**

RESEARCH OUTPUT *(Output Penyelidikan)*

D

NO OF PUBLICATION

KPI FOR NO OF PUBLICATION

	ISI	Scopus	Index Proceedings	Others
KPI	**1**	**2**	**1**	
Achievement	**3**	**-**	**1**	

The contribution of funder (UMP, MOHE, MOSTI, Industry etc.) as the fund provider must be acknowledged at all times in all forms of publications. Please state the grant number (RDU/UIC) and grant name.

	ISI	Scopus
Number of articles/ manuscripts/books *(Please attach the First Page of Publication)*	1. M.M. Hasan and M.M. Rahman. 2016. Performance and emission characteristics of biodiesel–diesel blend and environmental and economic impacts of biodiesel production: A review. Homogeneous Charge Compression Ignition Combustion: Advantages over Compression Ignition Combustion, Challenges and Solutions. Renewable and Sustainable Energy Reviews. 74: 938–948, (SCI Index, Q1, IF =6.798) 2. Hasan, M.M., Rahman, M.M., Kadirgama, K., Ramasamy, D. 2018. Numerical study of engine parameters on combustion and performance characteristics in n-heptane fueled HCCI engine. Applied Thermal Engineering, 128: 1464-1475. (WoS Indexed, IF: 3.771, Q1) 3. Hasan, M.M., Rahman, M.M., Nomani Kabir, M., Abdullah, A.A. 2017. Numerical Study on the Combustion and Performance Characteristics of an HCCI Engine Resulting from the Autoignition of Gasoline Surrogate Fuel. Journal of Energy Engineering, 143(5):4017049 (WoS Index, IF: 1.346, Q3)	1. H.Hanafi,, M.M.Hasan,, M.M.Rahman, M.M.Noor, K.Kadirgama and D. Ramasamy. 2016. Numerical modeling on homogeneous charge compression ignition combustion engine fueled by diesel-ethanol blends. MATEC Web of Conferences 74, 00037, 1-9.
Conference Proceeding *(Please attach the First Page of Publication)*	**International**	**National**

HUMAN CAPITAL DEVELOPMENT

KPI FOR HUMAN CAPITAL DEVELOPMENT

	PhD Student	Master Student
KPI		**1**
Achievement		**1**

Human Capital Development	**Number**				**Others** (please specify)
	On-going		**Graduated**		
Citizen	Malaysian	Non Malaysian	Malaysian	Non Malaysian	
PhD Student				1	
Masters Student					
Undergraduate Student					
Total				1	

Name of Student:	MOHAMMAD MEHEDI HASSAN
ID Matric No:	MMM14004
Faculty:	FACULTY OF MECHANICAL AND AUTOMOTIVE ENGINEERING TECHNOLOY
Thesis title:	NUMERICAL INVESTIGATION ON COMBUSTION, PERFORMANCE AND EMISSIONS CHARACTERISTICS IN HOMOGENEOUS CHARGE COMPRESSION IGNITION ENGINE
Graduation Year:	2016

INTELECTUAL PROPERTIES

KPI FOR INTELECTUAL PROPERTIES

Patent, Copyright, Trademark,Industrial Design: _____

Patent, Copyright, Trademark, Industrial Design ect	

OTHERS

KPI FOR OTHERS

Prototype, Technology,Collaborations etc: _____

Prototype, Technology, Collaborations etc	

ASSET *(Aset)*

E

Bil	**Peralatan** *(Equipment)*	**Model**	**No Daftar Aset** *(Asset Tagging No)*	**Amount** (RM)	**Lokasi** *(Location)*

PRODUCT DESCRIPTION FOR UMP R&D DIRECTORY (SHORT & BRIEF) *Only for Final Report*

F NOT APPLICABLE

PRODUCT PICTURE FOR UMP R&D DIRECTORY *Only for Final Report*

G NOT APPLICABLE

SUMMARY OF RESEARCH FINDINGS (*Ringkasan Penemuan Projek Penyelidikan)*

H

Biodiesels are gaining more importance as a promising alternative energy resource due to the global fossil fuel crisis and emission problems. However, it was realized that the extensive utilization of biodiesel would tax the food chain and could lead to food shortages. So, the use of a blend of biodiesel with conventional fuel was suggested to balance its usage, which could still provide a beneficial greenhouse effect. From the results of the investigation, it is reported that blends containing up to 30% biodiesel have almost the same properties as diesel. Most investigation results have shown that compared to diesel, biodiesel–diesel blend provides shorter ignition delay and a reduced heat release rate as well as a slightly higher efficiency by sacrificing a small amount of fuel. The HC, CO, and PM emissions are reduced to a great extent but the NOx emission becomes slightly higher. Biodiesels are expected to reduce the dependence on imported petroleum with the associated economic vulnerability, reduce greenhouse gas emissions and other pollutants, and revitalize the economy by increasing demand and prices for agricultural products. The objective of this study is to investigate the effect of intake temperature on combustion, performance and emissions characteristics in HCCI engine using pure *n*-heptane, the blends of *n*-heptane and ethanol fuels E15, E30 (including 15%, 30% ethanol and 85%, 70% *n*-heptane by vol. respectively) and the blends of *n*-heptane and butanol fuels Bu15, Bu30 (including 15%, 30% butanol and 85%, 70% *n*-heptane by vol. respectively) with the help of numerical simulation. In this study, neat diethyl ether (DEE), as well as diethyl ether and ethanol blends in different percentages by volumes such as 85% diethyl ether–15% ethanol (D85E15) and 70% diethyl ether–30% ethanol (D70E30), was used as test fuels. A zero dimensional single-zone numerical simulation with reduced fuel chemistry was developed and validated. The simulations show good agreement with the experimental data and capture important combustion phase trends as engine parameters are varied with a minimum percentage of error which is less than 6%. The simulations were run at the engine speed of 1200 rpm. The inlet air temperatures were selected as 360, 375, 390, 405 and 420 K and lambda values were taken as 1.5, 1.75, 2, 2.25 and 2.5. Simulation results show that HCCI combustion was advanced with the increase of intake temperature. Thermal efficiency was increased by about 17.71% with Bu30 compared to *n*-heptane at 393 K intake temperature. Indicated mean effective pressure decreased at all intake temperatures with *n*-heptane. Very low amount of NO_x emissions were measured with test fuels. NO_x emissions were increased with the increase of intake temperature. It is also seen that CO emissions were increased with the increase of alcohol in the test fuels. Higher HC emissions were obtained especially at lower intake temperature when ethanol was used as an additive fuel. Simulations results also show that increasing the lambda lowers the in-cylinder pressure and heat release rate for all test fuels. It was observed that the combustion phase was advanced and the combustion duration was prolonged with the increase of inlet air temperature. The starting of combustion was delayed with the increase of the amount of ethanol in the test fuel. Indicated mean effective pressure was increased by around 12.6% and was acquired as 6.10 bar for D85E15 when contrasted with D70E30 at $\lambda = 2$ and at 420 K inlet air temperature with the addition of ethanol. Indicated thermal efficiency was increased by around 11.4% and was acquired as 49.17% at $\lambda=2$ with DEE when contrasted with D85E15 at that lambda. Therefore, it was seen that diethyl ether and ethanol fuel mixes remarkably affected HCCI combustion and engine performance. As a result, it was found that the HCCI operation range can be extended using higher octane number alcohols and autoignition can be controlled

PROBLEMS / CONSTRAINTS IF ANY *(Masalah/ Kekangan sekiranya ada)*

I

Not applicable

Date :
Tarikh

Project Leader's Signature:
Tandatangan Ketua Projek

COMMENTS, IF ANY/ ENDORSEMENT BY FACULTY (*Komen, sekiranya ada / Pengesahan oleh Fakulti)*	
J	**Recommend / Not Recommend / KIV / Need Ammendment** .... **Name:** *Nama:* **Signature:** *Tandatangan:* **Date:** *Tarikh:* **** Dean/TDR/Director/Deputy Director**
COMMENTS, IF ANY/ ENDORSEMENT BY RMC PNI (*Komen, sekiranya ada / Pengesahan oleh RMC PNI)*	
K	**Recommend / Not Recommend / KIV / Need Ammendment** .... **Name:** *Nama:* **Signature:** *Tandatangan:* **Date:** *Tarikh:*

PROFILE BOOK
INTERNAL GRANT: RDU1503101

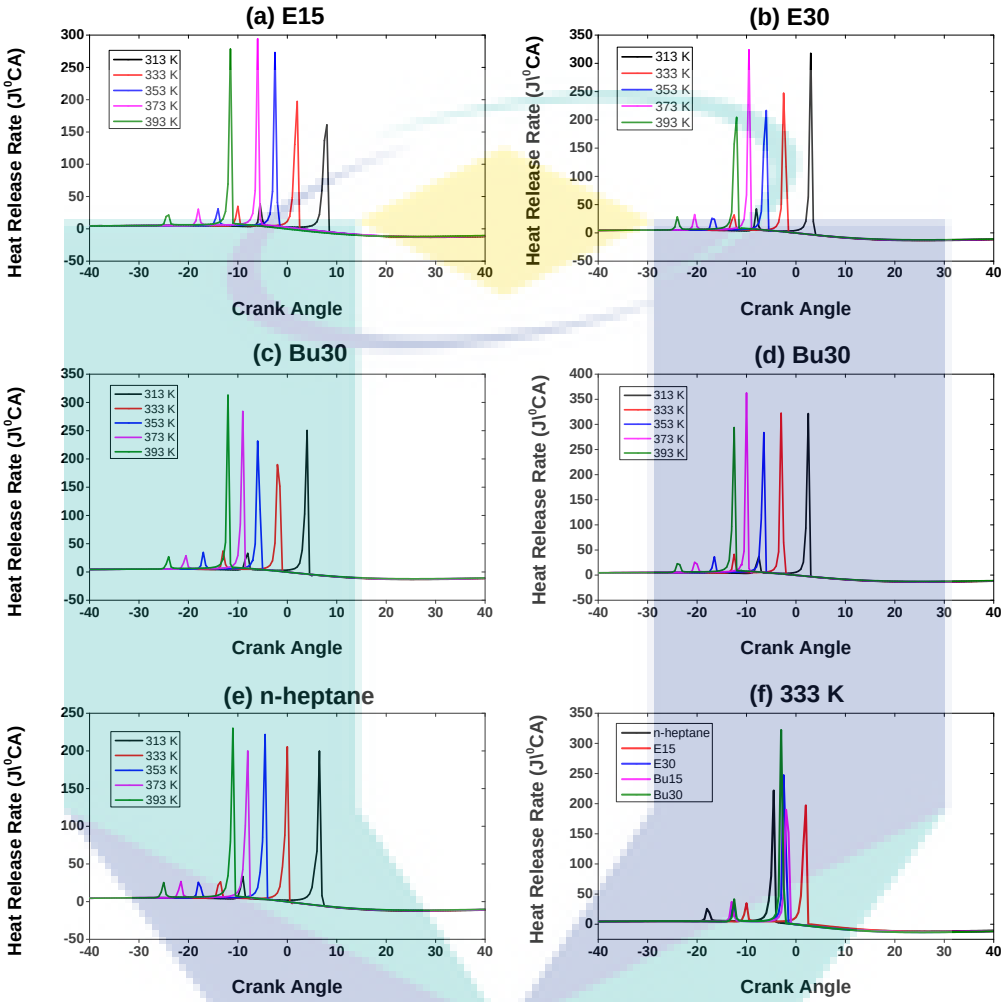

TITLE OF RESEARCH
BIODIESEL-DIESEL (UP TO 45%) FUEL CHARACTERISTICS ON HOMOGENEOUS CHARGE COMPRESSION IGNITION ENGINE

NAME OF PROJECT LEADER
PROFESSOR TS DR MD MUSTAFIZUR RAHMAN

NAME OF CO-RESEARCHERS
PM DR KUMARAN KADIRGAMA, FTKMA
PM DR DEVARAJAN RAMASAMY, FTKMA
PM DR WAN SHARUZI WAN HARUM, FTKMA
PROF. DR. RIZALMAN BIN MAMAT, FTKMA
DR. MUHAMAD MAT NOOR, FTKMA

AUTOMOTIVE ENGINEERING CENTRE
E-mail: mustafizur@ump.edu.my
Field: AUTOMOTIVE ENGINEERING

ABSTRACT

Biodiesels are gaining more importance as a promising alternative energy resource due to the global fossil fuel crisis and emission problems. However, it was realized that the extensive utilization of biodiesel would tax the food chain and could lead to food shortages. So, the use of a blend of biodiesel with conventional fuel was suggested to balance its usage, which could still provide a beneficial greenhouse effect. From the results of the investigation, it is reported that blends containing up to 30% biodiesel have almost the same properties as diesel. Most investigation results have shown that compared to diesel, biodiesel–diesel blend provides shorter ignition delay and a reduced heat release rate as well as a slightly higher efficiency by sacrificing a small amount of fuel. The HC, CO, and PM emissions are reduced to a great extent but the NOx emission becomes slightly higher. Biodiesels are expected to reduce the dependence on imported petroleum with the associated economic vulnerability, reduce greenhouse gas emissions and other pollutants, and revitalize the economy by increasing demand and prices for agricultural products. The objective of this study is to investigate the effect of intake temperature on combustion, performance and emissions characteristics in HCCI engine using pure *n*-heptane, the blends of *n*-heptane and ethanol fuels E15, E30 (including 15%, 30% ethanol and 85%, 70% *n*-heptane by vol. respectively) and the blends of *n*-heptane and butanol fuels Bu15, Bu30 (including 15%, 30% butanol and 85%, 70% *n*-heptane by vol. respectively) with the help of numerical simulation. In this study, neat diethyl ether (DEE), as well as diethyl ether and ethanol blends in different percentages by volumes such as 85% diethyl ether–15% ethanol (D85E15) and 70% diethyl ether–30% ethanol (D70E30), was used as test fuels. A zero dimensional single-zone numerical simulation with reduced fuel chemistry was developed and validated. The simulations show good agreement with the experimental data and capture important combustion phase trends as engine parameters are varied with a minimum percentage of error which is less than 6%. The simulations were run at the engine speed of 1200 rpm. The inlet air temperatures were selected as 360, 375, 390, 405 and 420 K and lambda values were taken as 1.5, 1.75, 2, 2.25 and 2.5. Simulation results show that HCCI combustion was advanced with the increase of intake temperature. Thermal efficiency was increased by about 17.71% with Bu30 compared to *n*-heptane at 393 K intake temperature. Indicated mean effective pressure decreased at all intake temperatures with *n*-heptane. Very low amount of NO_x emissions were measured with test fuels. NO_x emissions were increased with the increase of intake temperature. It is also seen that CO emissions were increased with the increase of alcohol in the test fuels. Higher HC emissions were obtained especially at lower intake temperature when ethanol was used as an additive fuel. Simulations results also show that increasing the lambda lowers the in-cylinder pressure and heat release rate for all test fuels. It was observed that the combustion phase was advanced and the combustion duration was prolonged with the increase of inlet air temperature. The starting of combustion was delayed with the increase of the amount of ethanol in the test fuel. Indicated mean effective pressure was increased by around 12.6% and was acquired as 6.10 bar for D85E15 when contrasted with D70E30 at $\lambda = 2$ and at 420 K inlet air temperature with the addition of ethanol. Indicated thermal efficiency was increased by around 11.4% and was acquired as 49.17% at $\lambda=2$ with DEE when contrasted with D85E15 at that lambda. Therefore, it was seen that diethyl ether and ethanol fuel mixes remarkably affected HCCI combustion and engine performance. As a result, it was found that the HCCI operation range can be extended using higher octane number alcohols and autoignition can be controlled

1. INTRODUCTION

The concern about fuel economy and emissions is increasing day by day because these are the basic issues for internal combustion (IC) engine industry. The primary emissions from IC engines are nitrogen oxides (NO_x), particulate matter (PM), unburned hydrocarbon (HC) and carbon monoxide (CO). Temperature is the main factor for the formation of NO_x. In conventional compression ignition (CI) and spark ignition (SI) engines, high temperature is produced during combustion because of the stoichiometric air-fuel mixture. Thus, NO_x cannot be averted in conventional IC engines. The reason for the formation of PM is similar to NO_x. When the high temperature and rich mixture exist together in the combustion process, certainly PM produces. Especially, PM emissions cannot be averted at high load condition. The incomplete combustion is the main reason for the production of UHC and CO in IC engines. In the exhaust stroke, the temperature remains comparatively low. Due to this, unburned fuel and combustion intermediate species cannot be consumed properly in this low-temperature zone. As a result, UHC and CO are produced which is very common phenomena for conventional IC engines. Great attention has been paid to the fuel consumption and thermal efficiency of IC engines. Reduction of fuel consumption diminishes the fuel supply and lessens the dependency on foreign sources of fuel and ultimately cost of fuel is positively affected [1].

The thermal efficiency of conventional IC engines is very low which is another concern for the automotive industry. It has been seen from research that a higher compression ratio can provide higher thermal efficiency [2, 3]. Therefore, future combustion systems should incorporate high efficiency, high compression ratio engines. However, the compression ratio of SI engines cannot be increased so much because the high compression ratio creates abnormal combustion with knock in SI engines [4]. To improve the performance of IC engines a number of initiatives have been taken out. Some modifications have been incorporated with IC engine to make it more energy efficient such as electric, fuel-cell or hybrid engines. The purpose of these technologies is to improve engine thermal efficiency as well as reduce engine emissions and fuel consumption throughout the lifespan of a vehicle. However, the implementation and commercialization of these technologies require a high cost which is the main obstacle of these new initiatives. Thus, alternative solving is necessary to improve the current IC engines with comparatively low development cost. One of the solutions is Homogeneous Charge Compression Ignition (HCCI). HCCI offers the potential of nearly undetectable NO_x and PM emissions while operating at high efficiency. HCCI combustion is defined as a process by which a homogeneous mixture of air and fuel is compressed until auto-ignition occurs near the end of the compression stroke [5]. SI engines have a spark plug to initiate the combustion with a flame front propagating across the combustion chamber. CI engines have a fuel injector to inject the diesel and the combustion takes place in a compressed hot air region. HCCI engines have no spark plug or fuel injector and the combustion starts spontaneously in multiple locations. High engine efficiency can be achieved with low NO_x and PM emissions. HCCI combustion is noticeably faster than either compression ignition or spark ignition combustion [6]. The comparison of different parameters influencing the combustion processes in SI, CI, and HCCI is given in Table 1.1. HCCI combustion can improve thermal efficiency and maintain low emissions as well as can be implemented by modifying either SI or CI engines [7]. A wide variety of fuels, a combination of fuels and alternative fuels can be used. Usually, a lean air-fuel mixture is used in HCCI engines. It ignites automatically in several locations and is then burned volumetrically without visible flame propagation

[8]. Once ignited combustion occurs very quickly and it is fully controlled by chemical kinetics rather than spark or ignition timing [9].

Table 1.1 Comparison of parameters influencing in SI, CI, and HCCI combustion engines [10]

Engine type	**SI**	**HCCI**	**CI**
Ignition method	Spark ignition	Auto-ignition	Compression ignition
Charge	Premixed homogeneous before ignition	Premixed homogeneous before ignition	In-cylinder heterogeneous
Ignition point	Single	Multiple	Single
Throttle loss	Yes	No	-----
Compression ratio	Low	High	-----
Speed	High	Low	-----
Combustion flame	Flame propagation	Multi-point auto-ignition	Diffusive flame
Fuel economy	Good	Best	Better
Max. efficiency	30%	>40%	40%
Major emissions	HC, CO, and NO_x	HC and CO	NO_x, PM, and HC
Injection type	Port injection	Port and direct injection	Direct injection
Equivalence ratio	1	<1	-----

The formation of NO_x and soot plays a significant role to understand the fundamentals of HCCI combustion. The regions of the formation of NO_x and soot have been illustrated in Figure 1.1. The formation of NO_x is a complex process that involves the reactive combination of nitrogen found within the combustion air and organically bound nitrogen within the fuel itself. NO_x is a thermally produced gas and therefore its formation is largely dependent on the control of the combustion temperature [10]. It is seen that at low equivalence ratios and high flame temperatures usually, NO_x formation occurs. The formation of NO_x can be reduced by keeping the flame temperature below 2200 K [11]. On the other hand, soot formation occurs in regions of high equivalence ratios or fuel rich mixtures and moderate temperatures. Net soot emission is a balance between formation and oxidation can be reduced either increasing mixing or increasing oxidation [12]. In conventional diesel engines, a representative fuel element would follow a path leading to both formations of both NO_x and soot emissions. Strategies to reduce NO_x formation during standard diesel operation normally lead to a penalty in soot emissions and vice versa. As both NO_x and soot emissions are strong functions of temperature and equivalence ratio, the most direct approach to reducing these emissions simultaneously is to carefully control the flame temperature and equivalence ratio [13]. In line with this approach, the main purposes of HCCI combustion are to concurrently lower the flame temperature and allow sufficient air and fuel mixing to increase the homogeneity of charge. From a conceptual point of view, when a thoroughly homogeneous in-cylinder mixture is formed, the pressure and temperature rise during the compression stroke resulted in simultaneous auto ignition across the whole cylinder. Local temperatures are maintained at low levels with the absence of a high-temperature flame front and NO_x

formation is thus avoided [14]. Soot formation is also avoided due to the homogenized lean mixture which lowers local equivalence ratios [15].

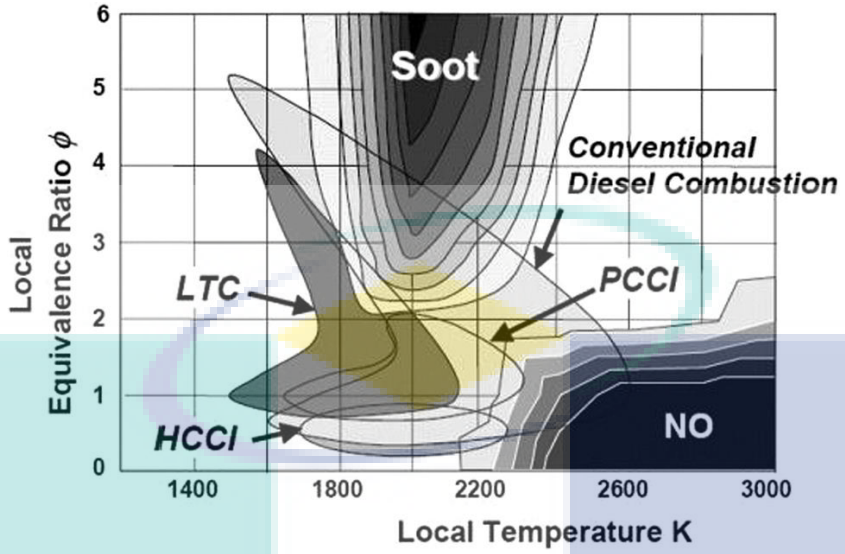

Figure 1.1. Equivalence ratios versus temperature (Soloiu, Duggan [16])

1.2 Problem Statements

HCCI represents an evolutionary step in case of thermal efficiency, fuel economy and emissions especially NO_x and PM compared to diesel and gasoline engines. However, differing from both of these traditional engines, HCCI engines lack a physical event which controls the ignition timing. It is the main challenge which ultimately influences the power and efficiency [17]. Unlike SI engines and CI engines, HCCI engines have no direct mechanism to control the start of combustion. Its start of combustion is fully dependent on auto-ignition. According to Yao, Zheng [18], this auto-ignition is affected by several factors like fuel auto-ignition chemistry and thermodynamic properties, combustion duration, wall temperatures, intake temperature and pressure, compression ratio, amount of EGR, engine speed, engine temperature, convective heat transfer to the engine, and other engine parameters. Higher intake temperatures and intake pressures cause earlier combustion timing due to the faster chemical kinetics [19]. For equivalence ratio sensitive fuels, higher equivalence ratios (up to stoichiometric) have a tendency to propel ignition timing due to the improvement of charge reactivity. The fuels without equivalence ratio sensitivity demonstrate an inverse pattern, where higher equivalence ratios have a tendency to bring about more delayed combustion timing. The lower specific heat ratio from higher equivalence ratios causes the prerequisite of more compression heating to achieve ignition temperatures. Nonetheless, in real operation, for both sorts of fuels the utilization of higher equivalence ratios likewise increases the in-cylinder wall and residuals temperatures, along these lines bringing on advanced combustion timing [20]. For fuels with little to no equivalence ratio sensitivity, there are contending impacts where lower specific heat ratios have a tendency to delay combustion while higher in-cylinder wall and residual temperatures have a tendency to propel combustion. To understand the effect of engine parameters on combustion, performance and emissions characteristics of HCCI engine, a fruitful study is needed which can be done by developing a more accurate simulation model based on zero-dimension and single zone rather than experiments or multidimensional modeling. Experimental work is costly and requires more time. Modeling is a way of exploring engine behavior in ways that might otherwise impossible in a true experimental approach. A multi-dimensional model requires substantial computational time as

compared to zero-dimensional and quasi-dimensional models, which are a simplified version of a multi-dimensional model [21]. Thus, the use of simplified model becomes increasingly important because of its advantages in computational time and resources. A zero-dimensional simulation would be an interim solution until the cost and time of running a multi-dimensional model is comparable with the current cost of the zero-dimensional model. The use of chemical kinetics mechanisms also helps in investigating the combustion behavior of an HCCI engine.

1.3 Objectives of Study

The objectives of this research are to investigate the influence of different engine parameters on combustion, performance and emissions characteristics in HCCI engines and to analyze the influence of different fuels and blends of fuels on combustion, performance and emissions characteristics in HCCI engines. The use of different fuels in HCCI engines, including diesel, gasoline, *n*-heptane and blends of *n*-heptane and ethanol as well as blends of *n*-heptane and butanol using 15% and 30% of both ethanol and butanol in blends. Collection of chemical properties of different fuels and blends of fuels from previously published literature. A study of the effects of engine speed, intake temperature and pressure and compression ratio by running simulation at engine speed ranging from 600 rpm to 1200 rpm, intake temperature ranging from 313 K to 393 K, intake pressure ranging from 100 kPa to 200 kPa and compression ratio ranging from 10 to 16 for diesel HCCI engine and at engine speed ranging from 600 rpm to 1800 rpm, intake temperature ranging from 373 K to 453 K, intake pressure ranging from 100 kPa to 200 kPa and compression ratio ranging from 12 to 16 for gasoline HCCI engine.

2. LITERATURE REVIEW

2.1 Effects of Engine Parameters

In order to develop an appreciable control method to optimize ignition timing and smooth heat release rate, it is very important to understand the effects of engine parameters on the ignition timing, combustion rate, performance and emissions (Lu et al., 2005). This section presents a review of the effects of different engine parameters such as intake temperature, intake pressure and compression ratio on HCCI engines using various fuels, with some brief discussion.

2.1.1 Intake Temperature

One of the main parameters to control HCCI combustion is the intake air temperature, which affects the time–temperature history of the mixture. High intake temperature advances the start of combustion but causes a reduction in the volumetric efficiency (Machrafi et al., 2010). Intake charge temperature affects the combustion and formation of emissions through two distinct pathways. When temperature is lowered, ignition delay is extended leading to enhanced air/fuel premixing. Additionally, the adiabatic flame temperature of a fuel parcel is decreased when it is mixed to a particular equivalence ratio. This means that fuel element is steered away from the NOx–soot formation region on the equivalence ratios–temperature map. Lu et al. (2005) found that the intake temperature plays the most sensitive influence on the HCCI combustion characteristics. They showed that the combustion phase was advanced, and the combustion duration was shortened with the increase of intake charge temperature. They also showed that increasing intake charge temperature from 31oC to 54oC increased NOx emissions linearly from approximately 10 ppm to 50 ppm when n-heptane fuel was combusted at fixed fuel delivery rate, engine speed and 30% EGR. This is in agreement with another HCCI work whereby NOx increased when inlet air temperature increased from 35oC to 80oC (Akagawa et al., 1999). Both unburned HC and CO were observed to be unaffected by intake temperature (Lu et al., 2005). Experiments conducted on a HSDI diesel engine revealed that peak soot luminosity were markedly reduced when intake temperature decreased from 110oC to 30oC under a load condition of 3 bar IMEP (Choi et al., 2005). This was attributed to both lower soot temperatures and reduced soot formation. Nonetheless, in-cylinder soot luminosity was clearly observed even at 30oC which indicated that complete eradication of soot formation was difficult with typical fuel injection system parameters.

2.1.2 Intake Pressure

Turbocharging is used in HCCI operation to extend the operating load range (Christensen and Johansson, 2000; Christensen et al., 1998a; Hyvönen et al., 2003). This is particularly relevant in HCCI operations whereby reasonably high EGR rates are typically employed to control combustion and limit NOx formation. The resulting dilution limits the amount of fuel that can be added for a fixed charge mass leading to a loss in engine power. To counter this for a given engine size, more mass needs to be forced through the engine through turbocharging. By supercharging to 86 kPa and increasing the fuel quantity at a lowered compression ratio of 12.5, the power output could be increased to nearly the full load of conventional, naturally aspirated diesel combustion. Similarly, in the premixed compression ignition combustion system, a boost pressure of 80 kPa produced an output which was comparable to that of the full load of conventional, naturally aspirated diesel combustion (Iwabuchi et al., 1999). Tests with n-heptane in a Cooperative Fuels Research engine operated in HCCI mode

showed that raising the intake pressure from approximately 117.5 kPa to 152.5 kPa resulted in a directly proportional increase in IMEP when all influential parameters such as compression ratio, intake charge temperature, EGR rate and equivalence ratio were kept constant (Hosseini and Checkel, 2007). In another study, turbocharging on a six-cylinder diesel engine achieved high loads of up to 16 bar BMEP with ultra-low specific NOx emissions (0.1 g/kW-hr) (Olsson et al., 2001). This compares to 21 bar BMEP for the same engine under standard diesel operation. Evaluation of boosting strategies for HCCI applications have been carried out by Olsson et al. (2004). The dilution required to limit NOx necessitates the use of much more boost compared to conventional engines for the same load. When high boost is required, turbocharger efficiency was presented to be very important for HCCI in order to reduce pumping losses. For high load applications, two stages turbocharging with inter-cooling is recommended. Better control of the turbocharger such as using variable geometry turbocharger avoids unnecessary pumping work through 'over boost'.

2.1.3 Compression Ratio

By lowering the compression ratio, ignition delay is prolonged which allows complete injection of all fuels prior to ignition, a prerequisite for premixed combustion and a reduction in the gas temperature of the combustion field at TDC of the compression stroke (Gan et al., 2011). Reducing compression ratio from 18:1 to 16:1 was part of the strategy used in the second generation of modulated kinetics diesel engines to extend low temperature, premixed combustion to higher load conditions (Raheman and Phadatare, 2004). It has been demonstrated by Olsson, Tunestål, Johansson, Fiveland, Agama, and Assanis (2002) that knock in HCCI diesel combustion can be prevented by reducing the compression ratio. When compression ratio is reduced, the accompanying reduction in temperature rise of the end gas prevents explosive self-ignition from occurring. Peng et al. (2005) conducted experiments on a four-stroke, single cylinder, variable compression ratio engine using n-heptane which verified the effects of compression ratio on HCCI combustion. The results showed that the possibility of knocking decreased, with the knock limit pulled to lower air fuel ratio region (richer mixture) when compression ratio was reduced from 18:1 to 12:1. The maximum IMEP attainable on this engine thus increased from 2.7 bar to 3.5 bar. Experiments carried out on a PCCI engine demonstrated that under premixed combustion, NOx emissions were only mildly reduced when compression ratio was reduced from 18.4:1 to 16.0:1 within the SOI timing range of 5oBTDC to 3oATDC (Laguitton et al., 2007). Soot emissions, unlike NOx, were reduced more markedly when compression ratio reduced. The reductions in NOx and soot emissions can be explained by the retardation in ignition delay which leads to a reduction in the gas temperature at TDC of the compression stroke and more complete mixing of air and fuel mixture.

2.2 Effects of Fuels and Additives

2.2.1 Effects of Fuels

Because of the restriction brought on by the combustion mode and engine set-up, conventional internal combustion engines must utilize particular fuels. For spark-ignition engines, gasoline is more appropriate due to having good volatility and anti-knock characteristics. On the other hand, for compression ignition engines, diesel is more appropriate due to having higher viscosity and lower resistance to auto-ignition (Valentino et al., 2012). Nonetheless, the HCCI combustion methodology can accommodate an assortment of fuel types as long as the fuel can be vaporized and mixed with air before ignition (Aceves and Flowers, 2004). Since ignition happens in an HCCI engine through auto-ignition of the air–fuel mixture, the selection of fuel

will have a huge effect on both the engine outline and the control procedures. Both fuel volatility and auto-ignition qualities are essential. Different fuels have different auto-ignition points. Figure 2.1 shows the intake temperature required for different fuels to auto-ignite at different compression ratios while operating in HCCI mode.

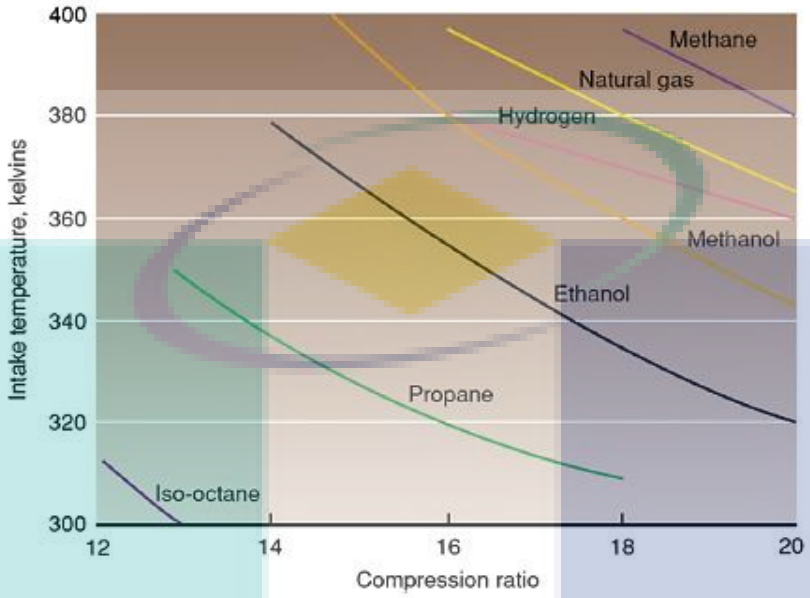

Figure 2.1 Intake temperature required for fuels to operate under HCCI mode with varying compression ratios (Aceves and Flowers (2004))

It is seemingly singular digress that the auto-ignition point decreases when the amid of carbon atoms in the hydrocarbon increases. According to Epping et al. (2002), to form a homogeneous charge easily the fuel must have a high volatility property. Chemically, fuels which have single-stage ignition react less with the change in load and speed. This helps the HCCI engine to run over a wide range of operating conditions. Christensen et al. (1999) concentrated on the relationship between the fuel's octane number, the inlet air temperature and the compression ratio expected to get auto-ignition near to TDC by blending iso-octane with octane number 100 and n-heptane with octane number 0. The test outcomes demonstrate that any fluid fuel can be utilized as a part of an HCCI engine utilizing a variable compression ratio. Diesel fuel auto-ignites more readily than gasoline. However, the non-premixed diesel engine is becoming a less suitable power production device due to the high NOx and soot emissions. Due to these challenges faced by the traditional diesel engine, diesel HCCI combustion gained lot of attention in the 1990s. Three different approaches were followed to achieve HCCI combustion with diesel fuel: premixed HCCI, early direct-injection HCCI, and late direct-injection HCCI. Ryan and Callahan (1996), followed by Gray and Ryan (1997), used the premixed HCCI approach in a single-cylinder, four-stroke, variable compression ratio engine. Fuel injectors introduced diesel fuel into the intake air stream and the mixture temperature was increased using an intake air heater. Compression ratio variation along with exhaust gas recirculation (EGR) was used to achieve HCCI. The study highlighted three issues with premixed diesel HCCI. First, premature ignition and knocking occurred if diesel compression ratios were used. Second, high intake temperatures were required to avoid the accumulation of liquid fuel on the surfaces of the intake system. Third, reduced combustion efficiency resulted in high HC emissions relative to traditional diesel operation. Several others (Christensen et al., 1999; Kaneko et al., 2002; Kelly-Zion and Dec, 2000; Suzuki et al., 1997) worked with premixed diesel HCCI and their results indicate that substantial reductions of NOx and soot emissions were achieved using this approach. However, it was also clear from these publications

that premixed diesel HCCI is not the best strategy for diesel-fuelled HCCI and alternative fuel-delivery or mixing techniques have to be developed. Early direct-injection (i.e. direct fuel injection well before TDC) is a favored diesel HCCI technique for two reasons. First, easy vaporization and better mixing is achieved when fuel is injected in hot compressed air during the compression stroke. Second, with an appropriately designed injector, fuel wall wetting can be minimized, which increases the combustion efficiency and reduces emissions. Several publications (Nakagome et al., 1997; Takeda et al., 1996; Walter and Gatellier, 2002; Yokota et al., 1997) reported using early direct injection to achieve diesel HCCI. Nissan Motor Company developed a process called modulated Kinetics that falls in the regime of late direct-injection diesel HCCI. The principles of this process were described by Mase et al. (1998) and Kimura et al. (1999). For this process, a long ignition delay period and rapid mixing was required, which assures premixed combustion and hence low smoke. Large amounts of EGR reduced the combustion temperature, resulting in low NOx. The ignition delay was also extended by increased EGR and retarded injection (near the top dead center, TDC). Rapid mixing was achieved by combining high swirl with improved combustion-bowl geometry. The modulated Kinetics process achieved low emissions with appropriate combustion control.

Gasoline has a lower boiling point and higher octane number. For this reason, using gasoline fuel in HCCI engines is the reason for early combustion, which limits the operating range of HCCI engines (Zhao, 2003). Ultimately, high combustion pressure and knock are created (Zhao, 2003). To solve these two major problems, delayed combustion is necessary. Several approaches have been used by many researchers (He et al., 2013; He et al., 2014b; Yeom et al., 2007). Yeom et al. (2007) used LPG with gasoline. LPG has a higher octane number than gasoline and it has a high latent heat of vaporization, which can bring down the compression pressure and temperature (Iida and Igarashi, 2000). In addition, LPG contains fewer carbon atoms than gasoline or diesel, and thus carbon dioxide (CO2) can be diminished by using LPG as part of the fuel mix in the engines (Campbell et al., 2004). Some scientists (Cedrone et al., 2011; He et al., 2013; He et al., 2014a, 2014b) blended n-butanol with gasoline to solve these problems. They observed that the onset of the auto-ignition occurs earlier and combustion duration becomes shorter when an increasing amount of n-butanol is used in place of gasoline. Other fuels besides gasoline and diesel are also used for HCCI engines. Since natural gas is the second most abundant fuel, many researchers have studied the feasibility of using natural gas (Christensen et al., 1997; Flowers, Aceves, Westbrook, et al., 2001; Hiltner et al., 2000; Olsson, Tunestål, Johansson, Fiveland, Agama, Willi, et al., 2002; Stanglmaier et al., 2001) as a fuel in HCCI engines. Due to the high octane rating of natural gas (of the order of methane, which has an octane rating of 107), high compression ratio (Christensen et al., 1999), high intake temperatures or additives promoting auto-ignition like NOx (Ricklin et al., 2002) and dimethyl ether (Chen et al., 2000) are required in natural-gas-fuelled HCCI engines. Performance aspects of propane-fuelled HCCI engines are discussed in (Au et al., 2001; Flowers, Aceves, Martinez-Frias, et al., 2001). Alcohols (Iida, 1994; Oakley et al., 2001) exhibit good auto-ignition properties and hence are excellent HCCI fuels, with a significantly larger operating range than most other fuels. Hydrogen is also studied as an alternative HCCI fuel (Shudo and Ono, 2002). In addition to the above-mentioned neat fuels, many fuel blends and additives like dimethyl ether, diethyl ether, dimethoxy methane or di-tertiary butyl peroxide (Eng et al., 2003) can be used in HCCI combustion.

2.2.2 Effects of Additives

Some chemical segments can advance the heat release process of auto-ignition. Along these lines, HCCI auto-ignition can be controlled by altering the fuel with the goal of making it more chemically responsive or inhibitive by including an ignition promoter or inhibitor. Christensen et al. (1999) and Iida et al. (2001) injected water into the fuel and observed a lower initial gas temperature. It was presumed that water injection can control the ignition timing and combustion duration. Verhelst and Wallner (2009) studied HCCI combustion using a hydrogen-enriched natural gas mixture. It was observed that hydrogen expansion in a natural gas mixture has the capacity to build in-cylinder peak pressure, reduce ignition delay time and ignition temperature, and expand indicated power (Raitanapaibule and Aung, 2005). It additionally permits the augmentation of the lean limit of the natural gas mixture, without entering the lean misfire region, while accomplishing amazingly low emissions (Verhelst and Wallner, 2009). Hydrogen expansion in ultra-low sulfur diesel advances incompletely premixed compression ignition and results in better performance and decreased emissions (Tsolakis and Megaritis, 2005). Szwaja and Grab-Logarinski (2009) considered hydrogen expansion (in HCCI mode) with diesel in a CI engine and found that the expansion of hydrogen in small amounts (e.g. about 5% in energy ratio) was able to diminish the ignition delay and enhance engine performance. They likewise reasoned that the expansion of hydrogen to diesel ought not to be more than 15% in energy ratio, to avoid extreme knock. (Shahbakhti and Koch, 2008) utilized a heptane/iso-octane mixture in an HCCI engine and found that this mixture is not suitable to control the ignition timing, but at low temperature the thermal efficiency was quite similar to that of a CI engine. Furthermore, formaldehyde-doped lean butane/air mixtures (Christensen et al., 1998b) exhibited ignition timing retardation and a decrease in combustion efficiency.

2.3 Numerical Study of HCCI Engines

In order to apply the actuators and sensors to a closed-loop HCCI combustion timing control system, it is useful to have a model for control analysis and synthesis. Modeling has been a focus of HCCI engine research for some time. Most of the models are based on chemical kinetics and not suitable for control analysis or synthesis. Zhao (2003) provided an extensive summary of these models and categorize them into zero-dimensional single-zone thermo-kinetic models, quasi-dimensional models that include some geometric effects and computational fluid dynamic (CFD) based multi-zone models. These types of models are complex and usually focus on producing a single cycle of data. For control analysis and synthesis, a model capable of quickly simulating seconds or even minutes worth of data is desirable.

2.3.1 Chemical Kinetics

In a CI engine, the fuel is direct-injected in the chamber with a high injection pressure when the piston is nearly at TDC. Then, the fuel ignites rapidly in the hot air environment. In SI engines, the spark plug is triggered when the piston is approximately at TDC to initiate the combustion. HCCI engines, on the other hand, have no mechanism to control the ignition timing and rely solely on chemical kinetics for combustion. The combustion in an HCCI engine is triggered when the heat in the chamber has reached the fuel activation energy. To numerically investigate the combustion behavior, chemical kinetic mechanisms which represent the actual fuels have been developed (Curran et al., 1998; Lee et al., 2010; Mehl, Pitz, et al., 2011). It is common to use n-heptane as a surrogate fuel for diesel (Guo et al., 2010;

Hernandez et al., 2008; Pitz and Mueller, 2011; Westbrook et al., 2006) because the chemical properties between those two are very similar, particularly in terms of cetane number. The intake temperature when n-heptane is used as a fuel in an HCCI engine is not as high as methane or natural gas. A study by Guo et al. (2010) showed that n-heptane can easily be ignited when the inlet temperature is 313K on a low CR engine (CR=10). Methane, on the other hand, is reported to have no ignition when the inlet temperature is less than 400K on a high CR engine (CR=15) (Fiveland and Assanis, 2000). Thus, it is important to have the right fuel and its chemical kinetic mechanism in order to study the combustion behavior of an HCCI engine. Curran et al. (1998) developed a detailed mechanism for n-heptane and validated the result over a wide range of operating conditions. They found that the ignition delay is in very good agreement with experiments using flow reactors, shock tubes and rapid compression machines. Seiser et al. (2000) and Ogink and Golovitchev (2002) developed a reduced mechanism for n-heptane because a detailed mechanism uses more computational resources. Patel et al. (2004) reduced the mechanism by more to obtain 26 species and 52 reactions. The author reported that the CPU time is reduced by 50-70% and the validation was completed under both constant-volume reactor and HCCI engine conditions. The ignition delay result is similar to those of detailed mechanisms. The use of n-heptane as the only main component in the mechanism is not sufficient to predict the soot emission from CI and HCCI engines. Thus, Wang et al. (2013) improved the mechanism by blending the n-heptane and toluene mechanisms. They reported that the mechanism gives reliable soot predictions and combustion phasing under various engine conditions. An iso-octane mechanism was used as a surrogate fuel for gasoline and it can also be blended with n-heptane to represent a real fuel (Curran et al., 2002; Tanaka et al., 2003). A real gasoline fuel consists of thousands of hydrocarbon compounds (Ogink and Golovitchev, 2001; Zheng et al., 2002) and the fuel should be modeled using a combination of a few components. Mehl, Pitz, et al. (2011) developed a mechanism that represents a commercial grade gasoline, which consists of n-heptane, iso-octane, toluene and olefins. They reported that the result is in good agreement over a wide range of pressures and temperatures relevant to internal combustion engine applications. A reduced mechanism was also developed by Mehl, Chen, et al. (2011) and further reduced by (Kwon et al., 2011). A reduced mechanism shows an advantage when used in a complex CFD model, which requires more computational resources (Lee et al., 2010).

2.6.1 Single Zone Model

A single-zone model is where the combustion chamber area is treated as one homogeneous block. The single-zone model has some limitations due to the assumption that the whole combustion chamber is treated as homogeneous (Fiveland and Assanis, 2001). Peak cylinder pressure and rate of pressure rise can be over-predicted. It also predicts a short burn duration and cannot accurately predict CO and HC emissions, which primarily depend on crevices (Su, 2010). Crevices and the boundary layer are the cold areas for HC and CO to react during combustion. The earliest example of this type of model was developed by Najt and Foster (1983) to help analyze experimental work on a premixed-charge, compression-ignited CFR engine. Their model employed the Shell ignition model and an empirical Arrhenius single step combustion model. By fitting the model constants to a wide range of engine combustion rate data, the authors were able to suggest that the combustion process was dominated by kinetics, a view that is widely accepted today. Recent examples of zero-dimensional models use more sophisticated and detailed chemical kinetics (Aceves, Flowers, Martinez-Frias, Smith, Westbrook, et al., 2001; and Dec, 2002). In general, these models have been successful in exploring the effects of fuel composition, compression ratio, air-fuel ratio, EGR rates and other operating

parameters, as well as the lean limits of HCCI operation. Ogink and Golovitchev (2001) have combined the single zone approach with existing zero-dimensional engine models to provide accurate estimates of the effects of the gas exchange process and have used the resulting simulations to evaluate unconventional engine concepts or variable valve timing strategies. Fiveland and Assanis (2000) proposed a full cycle, thermo-kinetic single zone model. The fresh charge was assumed to be perfectly homogeneous, with fluid mechanics assumed to have no impact on combustion phasing and rate besides their effect through cylinder wall heat transfer. Detailed chemical kinetics mechanisms for natural gas were applied to predict the ignition timing and heat release rate. Their model contributed to understanding how mixture preparation and in-cylinder thermodynamics conditions affect ignition timing, as well as engine performance. While the zero-dimensional, single zone, thermo-kinetic models have presented the ability to yield satisfactory accuracy against measurements of engine performance, they suffer significant shortcomings in predicting the rate of heat release, combustion completeness, and emissions, largely due to the simplifying assumption of strict homogeneity throughout the combustion chamber. Inaccurate estimates of residual temperature and species composition critically affect predictions of subsequent cycles, temperature and species composition critically affect predictions of subsequent cycles, thus limiting the ability of the simulation to track transients. Thus, this type of model cannot be directly used as a control and design tool, despite its computational efficiency. The potential problem of this type of model is to expand the engine operating range into an unrealistic region.

2.4 Summary

Engine parameters like intake temperature and pressure, compression ratio etc. as well as fuels and blends of fuels have great significance to achieve successful HCCI operation. However, HCCI engines still have unsolved issues, which are ignition control, knocking and high levels of unburned HC and CO emissions. Further studies have to be performed in order to solve these remaining issues. To achieve this, the numerical method shows a great advantage over experiments to simulate combustion behavior in terms of cost and time. To this end, a simulation model has to be developed to investigate the behavior and, once completed; it has to be validated against experiments. In this thesis, zero-dimensional single model was chosen for modeling a HCCI engine. A zero-dimensional model requires less computational time compared to multi-dimensional model. Thus, a zero-dimensional simulation would be an interim solution until the cost and time of running a multi-dimensional model is comparable with the current cost of the zero-dimensional model. The use of chemical kinetics mechanisms also helps in investigating the combustion behavior of an HCCI engine. The details of the modeling will be discussed in Chapter 3.

3. METHODOLOGY

3.1 NUMERICAL MODELING

Modeling combustion engines using computer codes is an important investigative technique. There are a number of different factors to be considered when developing a numerical model - chemistry, heat transfer, mechanical behavior, and fluid dynamics to name a few. In this study, a zero-dimensional single zone model for HCCI engine was established using MATLAB. The model is called zero-dimensional model because time is the only independent variable used in this model. The proposed method takes into account the detailed thermodynamic aspects of engine. The model integrates the ordinary differential equation system corresponding to the chemical and thermal evolution of a closed homogeneous system under an imposed volume history reproducing the engine cycle. This single-zone in time model treats the cylindrical combustion chamber as a uniform reactor with uniform temperature, pressure, and composition throughout. The reactor volume changes based on slider-crank relations that determine the motion of the piston in the engine cylinder. This kind of model aims to simulate the auto-ignition process in the core of the air-fuel mixture and enables the use of detailed chemical kinetic models with which we can investigate the chemical reactions contributing to cylinder inside pressure and temperature. The accumulated gas is assumed to be ideal gas. The models used two different types of chemical reaction mechanisms to model the fuels because two types of engine configurations were used. This is to ensure that the model works in both engine conditions. This Chapter will describe chemical kinetics mechanisms for diesel, gasoline and other test fuels first as well as emissions formation. Then the equations used in zero-dimensional single zone modeling will be presented in detail. To understand how the numerical code works an algorithm flow chart will be presented. Combustion and performance parameters will be described in brief. At the end of the Chapter chemical properties of the test fuels will be presented.

3.1.1 Chemical Kinetics Mechanisms

A combustion event involves an extraordinary amount of elementary chemical reactions. Each reaction has a designated pre-exponential term (A, $l/cm^3mol^{-1}sec^{-1}$), temperature dependent exponent (*b*, no units), and activation energy (E_A, in kJ/mol) which are used to describe the reaction rate coefficient (k) according to Eq. (3.1).

$$k = AT^b \exp\left(\frac{-E_A}{RT}\right) \tag{3.1}$$

The development of chemical mechanisms for numerical modeling is ongoing research. The researchers are testing, refining, and updating the values. Validation through comparisons with experimental results from shock tube and rapid compression machine experiments is one of the appropriate approaches. These mechanisms which can include on the order of 1000's of species (in the case of diesel fuel, for example) can quickly become cumbersome when running complex models. Therefore, another approach in the development of chemical mechanisms focuses on coming up with smaller mechanisms which still provide a desired degree of accuracy. This is done by constraining the conditions considered in the validation steps so that certain intermediate species and reactions can be ignored. These smaller mechanisms are often called skeletal or reduced mechanisms, with reduced mechanisms being the most drastically constrained and application-specific.

3.1.2 Diesel Mechanism

A chemical reaction mechanism is used to solve the chemical reactions during combustion. For diesel fuelled HCCI engines, a reduced diesel fuel surrogate mechanism [22] was used to simulate the diesel combustion. Pei and his co-workers assembled a kinetic mechanism describing the oxidation of n-dodecane/m-xylene mixture based on recently published kinetic mechanisms developed by the Lawrence Livermore National Laboratory. The detailed multi-component mechanism for n-dodecane and m-xylene was developed by combining the previously developed n-dodecane mechanism [23] with a recently developed mechanism detailing the combustion of the xylene isomers [22]. The two parent mechanisms were individually validated against an extensive set of experimental data for both fuels, including ignition delay time, speciation and laminar flame speed data. The detailed mechanisms, containing 2885 species and 11754 reactions, has been reduced using a combination of directed relation graph with expert knowledge [24] and directed relation graph aided sensitivity analysis algorithms coupled with isomer lumping. The resulting mechanism, including 163 species and 887 reactions, has been successfully applied to the simulation of 3D diesel-like spray combustion using a commercially available CFD code. This reduced mechanism for diesel surrogate was used in this study.

3.1.3 Gasoline Mechanism

In this study, a 4-component surrogate was used to model gasoline fuel. This surrogate was developed by Mehl, Chen [25] at Lawrence Livermore National Laboratory. The surrogate is comprised of isooctane, *n*-heptane, toluene and 2-pentene, and the relative proportion of each component by a mass fraction is given in Table 3.1.

Table 3.1 Gasoline surrogate composition

Component	Mass fraction
iso-octane	0.5413
n-heptane	0.1488
Toluene	0.2738
2-pentene	0.0361

In order to determine the composition of the surrogate, Mehl and coworkers used both composition of real gasoline (in terms of aromatics, olefins, alkanes and average molecular weight) as well as reactivity of gasoline (autoignition properties) to formulate a surrogate having a similar overall representation of various kinds of hydrocarbons and having similar (RON + MON)/2 as gasoline where RON stands for Research Octane Number and MON stands for Motor Octane Number. The choice of isooctane, *n*-heptane and toluene has been attributed to historical reasons, since they fit well within the molecular weight range of interest, and have been traditionally well understood within the combustion community. The addition of 2-pentene to represent olefins has been attributed to this molecule matching the typical molecular weight of olefins found in gasoline, and also because it has the highest octane number and sensitivity. A detailed chemical kinetic mechanism for this surrogate was developed by Mehl, Pitz [26], which consists of roughly 1400 species and 5000 reactions. This mechanism was validated against gasoline shock tube data over a range of temperatures and pressures. However, it is computationally infeasible to incorporate such a large mechanism within a 3-D CFD simulation; hence the same group [25] also

developed a reduced 312-species, 1488-reaction chemical kinetic mechanism based on the detailed mechanism, intended for 3-D CFD simulation of HCCI engines. This model was validated against HCCI engine experiments by Mehl, Pitz [27] over a range of intake pressure and load conditions, and was found to capture features such as intermediate temperature heat release [28] which are thought to be unique to gasoline fuel chemistry at higher pressures near TDC. This 312-species mechanism along with the 4-component gasoline surrogate was used in this study.

3.2 Mechanisms for Different Fuels and Blends of Fuels

A reduced *n*-heptane mechanism [29] was used to simulate *n*-heptane fuel in the HCCI combustion. The mechanism consists of 159 species and 770 elementary reactions. For *n*-heptane/ethanol blend fuel a reduced ethanol mechanism was combined with the *n*-heptane mechanism [30]. The final mechanism consists of 167 species and 1591 elementary reactions. In addition, for *n*-heptane/butanol blend fuel a reduced *n*-butanol mechanism was combined with the *n*-heptane mechanism [31]. The final mechanism consists of 181 species and 1703 elementary reactions.

3.2.1 Mechanism of Emissions Formation

Exhaust emissions consist mainly of direct combustion products, such as water and carbon dioxide, and pollutants such as CO, UHC and NO_x (which refers to the combination of NO and NO_2). The CO and UHC pollutants are a consequence of incomplete combustion. With rich air-fuel mixtures there is not enough oxygen to ensure oxidation of the carbon in the fuel to CO_2, also the carbon monoxide oxidation also freeze with the drop in temperature during the expansion stroke. To improve drivability during cold starts, the fuel flow is increased to compensate for slow fuel vaporization. However, this strategy leads to an increase in CO emissions as well as UHC. The CO formation can be summarized in the following reaction,

$$RH \rightarrow R \rightarrow RO2 \rightarrow RCHO \rightarrow RCO \rightarrow CO$$

where R is the hydrocarbon radical. The carbon monoxide formed is then oxidized to carbon dioxide at a slower rate via the principal oxidation reaction,

$$CO + OH \longleftrightarrow CO2 + H$$

There are several ways leading into the formation of unburned hydrocarbons. Due to the increasing cylinder pressure forces during the compression stroke part of the air-fuel mixture is trapped into the crevices, this mixture will not be exposed to the high temperatures and it will remain unburned. These unburned gases will then leave the crevices during exhaust stroke. Other sources of formation of UHC are the cold cylinder walls that lead to flame termination before the completion of the oxidation reactions. Engine oil left in thin films on the cylinder wall and piston can absorb and desorbs hydrocarbons before and after combustion, contributing as well to the formation of UHC.

The formation of NO_x is a complex process that involves the reactive combination of nitrogen found within the combustion air and organically bound nitrogen within the fuel itself. NO_x is a thermally produced gas and therefore its formation is largely dependent on the control of the combustion temperature. There are many other mechanisms from which NO_x can be produced, but thermal and prompt NO are more relevant in the internal combustion engines application [13, 32-34].

In the combustion of clean fuels (fuels not containing nitrogen compounds), oxidation of atmospheric nitrogen by the thermal mechanism is a major source of NO_x emissions. The three principal reactions that comprise the thermal NO formation mechanism are,

$$O + N2 \longleftrightarrow NO + N$$

$$N + O2 \longleftrightarrow NO + O$$

$$N + OH \longleftrightarrow NO + H$$

The first two reactions compose a chain sequence in which a small amount of atomic oxygen can produce large amounts of NO. This mechanism, often called the Zeldovich mechanism, is very sensitive to temperature not only because the high activation energy of the first reaction, but also because the concentration of oxygen atoms in flames increases rapidly with increasing temperature [13, 32-34].

Nitric oxide formation rates in combustion of hydrocarbon fuels can exceed those attributable to the thermal mechanism discussed above, especially for fuel-rich conditions. This rapidly formed NO was termed prompt NO, since it's rapid and is confined to regions near the flame zone.

$$CH + N2 \longleftrightarrow HCN + N$$

$$CH2 + N2 \longleftrightarrow HCN + NH$$

$$CH2 + N2 \longleftrightarrow H2CN + N$$

$$C + N2 \longleftrightarrow CN + N$$
$$N + O2 \rightarrow NO + O$$

$$N + OH \rightarrow NO + H$$

It has been shown that, prompt NO in hydrocarbon flames is formed primarily by a reaction sequence of hydrocarbon radicals with molecular nitrogen, leading to formation of amines or cyano compounds that subsequently react to form NO. Numerous studies showed that CH and CH_2 are the hydrocarbon radicals that most contribute to the formation of prompt NO [13, 32-34].

In HCCI, combustion occurs through chemical oxidation, thus, the reached maximum temperature is determined by the energy content of the fuel/air/residuals mixture, giving lower maximum temperatures than comparable with SI or CI. While the Zeldovich mechanism (thermal NO) is adequate for calculating NO_x emissions in SI or CI engines, it is safe to say that it doesn't accurately predict these emissions on HCCI combustion. Studies on lean combustors showed that NO_x is largely formed through N_2O paths. It appears believable that N_2O reaction pathways would play an important role in NO_x formation also for HCCI engines [13, 32-34]. To predict the NO_x formation accurately, a NO_x mechanism prepared by Miller and Bowman [13] was integrated with all the mechanisms. For this reason, 7 extra species were added. The species are NO, NO_2, NO_3, N_2O, HONO, HNO, and CH_3O_2. Ultimately, 27 reactions were added with all the mechanisms. The reaction rates for all the reactions were taken from Miller and Bowman [13] and Mueller, Yetter [35]. For completeness, the added NO_x mechanism reaction rates are summarized in Table 3.2.

Table 3.2 NO_x kinetic mechanism reaction rates parameters for *A*, *b*, and E_A

S/L	Reaction (cm^3 – mol – sec – cal - k)	*A*	*b*	E_A
1	NO+O(+M)=NO2(+M)	3.00E+13	0.00	0.0E+00
2	NO+H(+M)=HNO(+M)	1.52E+15	-0.41	0.0E+00
3	NO+OH(+M)=HONO(+M)	1.10E+14	-0.30	0.0E+00
4	NO2+H2=HONO+H	0.733E+12	0.0E+0	2.881E+04
5	NO2+O=O2+NO	1.05E+14	-0.52	0.0E+00
6	NO2+O(+M)=NO3(+M)	1.33E+13	0.00	0.0E+00
7	NO2+H=NO+OH	1.32E+14	0.00	3.62E+02
8	HO2+NO=NO2+OH	2.11E+12	0.00	-4.790E+02
9	NO2+NO2=NO3+NO	9.64E+09	0.73	2.092E+04
10	NO2+NO2=2NO+O2	1.63E+12	0.00	2.612E+04
11	HNO+H=NO+H2	4.4E+11	0.72	650.0
12	HNO+O=OH+NO	1.81E+13	0.00	0.0E+00
13	HNO+OH=H2O+NO	1.30E+7	1.88	-956.0
14	HNO+NO=N2O+OH	2.00E+12	0.00	26000.0
15	HNO+NO2=HONO+NO	6.02E+11	0.00	1.987E+03
16	HNO+HNO=H2O+N2O	8.51E+08	0.00	3.080E+03
17	HONO+O=OH+NO2	1.20E+13	0.00	5.961E+03
18	HONO+OH=H2O+NO2	1.7E+12	0.00	-5.200E+02
19	N2O(+M)=N2+O(+M)	7.91E+10	0.00	56,024
20	N2O+O=O2+N2	1.00E+14	0.00	2.80E+04
21	N2O+O=NO+NO	1.00E+14	0.00	2.80E+04
22	N2O+H=N2+OH (DUP)	2.53E+10	0.00	4.550E+03
23	N2O+H=N2+OH (DUP)	2.23E+14	0.00	1.675E+04
24	N2O+OH=HO2+N2	2.0E+12	0.00	40000.0
25	NO+N2O=NO2+N2	1.0E+14	0.00	50000.0
26	CH3O2+NO=CH3O+NO2	2.530E+12	0.00	-358.00
27	CH3+O2(+M)=CH3O2(+M)	1.006E+08	1.630	0.00

3.3 Engine Parameters

The engine movements are defined from the engine parameters, which have to be defined before employing the energy equation of the first law of thermodynamics in the zero-dimensional model. Figure 3.1 presents the geometry of the piston and crank mechanisms. The crank radius (*a*) is defined as half the stroke length (*L*) which is expressed in Eq. (3.2)

$$a = \frac{L}{2} \tag{3.2}$$

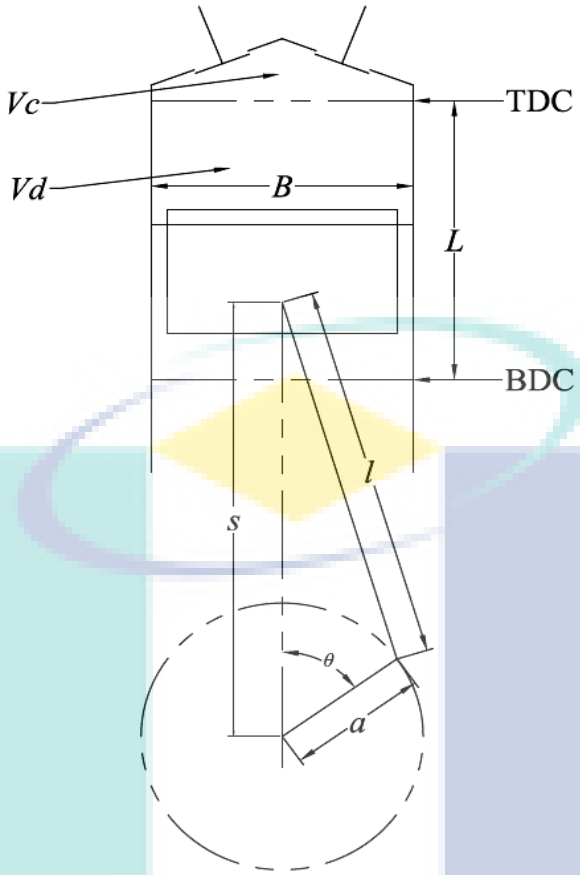

Figure 3.1 Engine geometry of the piston and crank mechanisms (Heywood [36])

The ratio of connecting rod length to crank radius is given by Eq. (3.3)

$$R = \frac{L}{a} \tag{3.3}$$

The rotational speed of the engine is expressed by Eq. (3.4)

$$\omega = \frac{2\pi N}{60} \tag{3.4}$$

where N is the engine speed in rotations per minute (RPM).
For a flat piston crown, the area is given by Eq. (3.5)

$$A_p = \frac{\pi B^2}{4} \tag{3.5}$$

where B represents the bore diameter of the engine.
When the piston is at TDC, the clearance volume is defined as Eq. (3.6)

$$V_c = \frac{V_d}{(R_c - 1)} \tag{3.6}$$

where V_d is the displacement volume and R_c is the compression ratio, which are given as

$$V_d = A_p L \tag{3.7}$$

$$R_c = \frac{maximum cylinder\ volume}{minimum cylinder\ volume} = \frac{V_d + V_c}{V_c} \tag{3.8}$$

From these parameters, the instantaneous piston speed can be obtained from Eq. (3.9)

$$S_p = \frac{\pi}{2}\overline{S_p}\sin\theta\left(1 + \frac{\cos\theta}{\sqrt{R^2 - \sin^2\theta}}\right) \tag{3.9}$$

where $\overline{S_p}$ is the mean piston speed.

The mean piston speed can be defined as Eq. (3.10)

$$\overline{S_p} = \frac{2LN}{60} \tag{3.10}$$

The instantaneous piston speed is zero at the beginning of the stroke and approaches its maximum at the middle of the stroke. It goes to zero again at the end of the stroke, as shown in Figure 3.2.

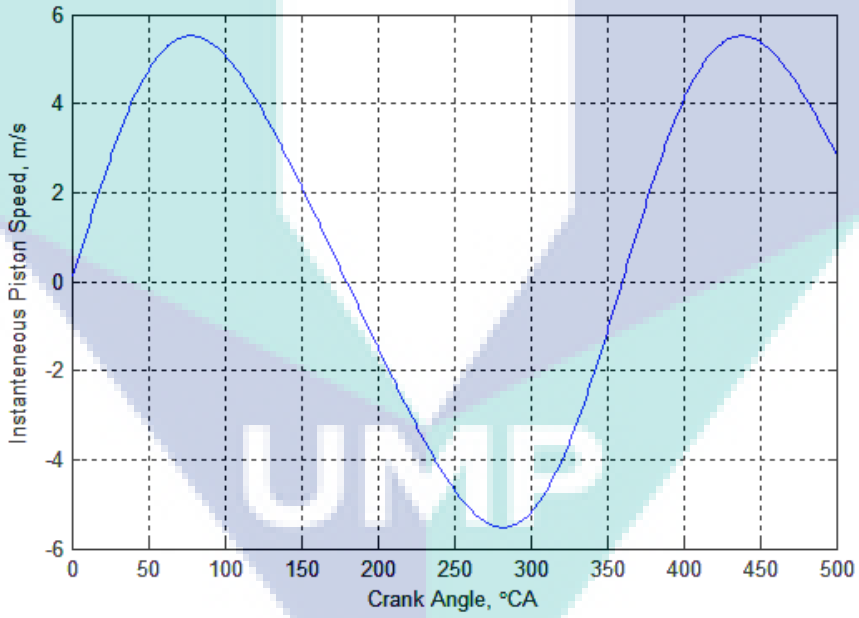

Figure 3.2 Instantaneous piston speed: zero at TDC and BDC, maximum at the middle of the stroke

The instantaneous cylinder volume at any crank angle location can be determined by Eq. (3.11)

$$V = V_c + A_p(l + a - s) \tag{3.11}$$

where s is the distance between crank axis and piston pin axis, which is given by Eq. (3.12)

$$s = a\cos\theta + \sqrt{(l^2 - a^2\sin^2\theta)} \tag{3.12}$$

After manipulation of Eqs. (3.11) and (3.12), the instantaneous cylinder volume is expressed as Eq. (3.13)

$$V = V_c\left[1+\frac{R_c-1}{2}\left(R+1-\cos\theta-\sqrt{R^2-\sin^2\theta}\right)\right] \tag{3.13}$$

The rate of change of volume can be expressed by Eq. (3.14)

$$\frac{dV}{d\theta} = V_c\left[\frac{R_c-1}{2}\left(\sin\theta\right)\left(\frac{1+\cos\theta}{\sqrt{R^2-\sin^2\theta}}\right)\right] \tag{3.14}$$

Cylinder volume is an important parameter because it determines the piston work in the energy equation.

3.4 Valve Geometry

Valve geometry is an important parameter to be considered because the mixing begins in the inlet manifold and it determines the mass flow rate to the combustion chamber. In engine configurations, the valve head is circular with a slightly different diameter between inlet and exhaust valves. Typical valve geometry for most engines is shown in Figure 3.3.

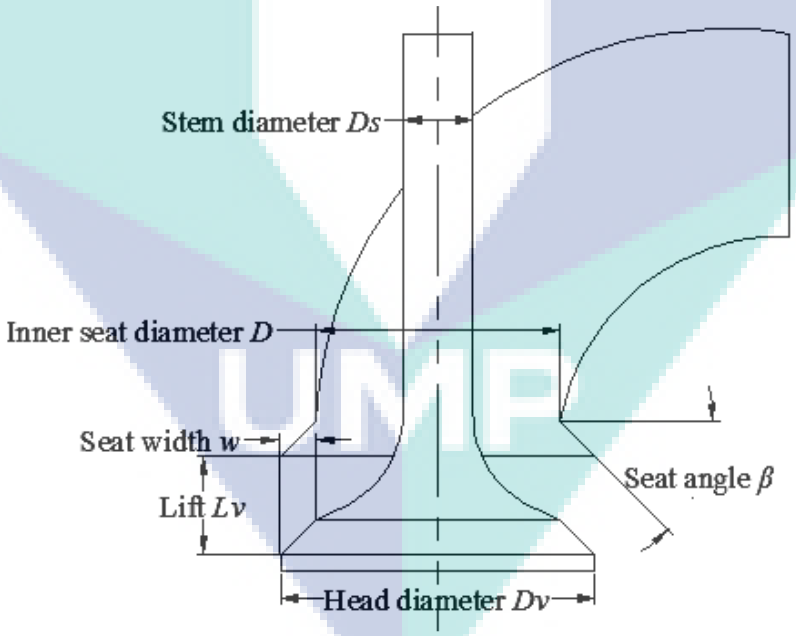

Figure 3.3 Valve geometry for most engines with parameters defining the valve (Heywood [36])

Based on Heywood's definition [36] on valve configurations for most engines, the valve head diameter is taken as

$$D_v = 1.1D \tag{3.15}$$

where D is the inner seat diameter, as shown in Figure 3.3. Then, the valve seat width is

$$S_w = D_v - D \tag{3.16}$$

with the valve stem diameter defined as

$$D_s = 0.2D \tag{3.17}$$

In order to determine the mass flow rate of the mixture to the combustion chamber, the valve lift profile has to be defined. The valve lift profile is determined by using the desired maximum valve lift (L_v) and half-event angle (c). The half-event angle is defined as half of the total valve opening duration. The profile as a function of crank angle [37] is then given by Eq. (3.18).

$$y = L_v + C_2\theta^2 + C_w\theta^w + C_q\theta^q + C_r\theta^r + C_s\theta^s \tag{3.18}$$

where w, q, r and s are constants to match the desired valve lift curve, which are selected as $w = 6$, $q = 8$, $r = 10$ and $s = 12$.

$$C_2 = \frac{-wqrsL_v}{[(w-2)(q-2)(r-2)(s-2)c^2]} \tag{3.19}$$

$$C_w = \frac{-wqrsL_v}{[(w-2)(q-2)(r-2)(s-2)c^2]} \tag{3.20}$$

$$C_q = \frac{-2wrsL_v}{[(q-2)(q-w)(r-q)(s-q)c^q]} \tag{3.21}$$

$$C_r = \frac{-2wrsL_v}{[(r-2)(r-w)(r-q)(s-r)c^r]} \tag{3.22}$$

$$C_s = \frac{-2wqrsL_v}{[(s-2)(s-w)(s-q)(s-r)c^s]} \tag{3.23}$$

Using Eq. (3.18), a typical valve lift profile with tappet mechanism (mechanical lifters) is illustrated in Figure 3.4 [36]. Once the valve lift is known, the effective valve open area can be obtained. In this case, the effective valve open area is taken as its curtain area, which is given by

$$A_c = \pi D_v L_v \tag{3.24}$$

Figure 3.4 presents a typical profile of valve lift for poppet valves with mechanical lifters. Generally, larger valve sizes (or more valves per cylinder) give higher maximum air flow in and out of the chamber. The mass flow rate to the combustion chamber can be obtained by using the equation of compressible flow through a flow restriction [36]. The equation includes the real gas flow effects with discharge coefficient C_d obtained from the experiments. In principle, the mass flows in or out of the combustion chamber when there is a pressure difference between the chamber and ports. The equation is separated into two cases: choked and subsonic flows. For choked flow, the following conditions are obeyed:

$$\frac{p_T}{p_0} \le \left[\frac{2}{\gamma+1}\right]^{\frac{\gamma}{\gamma+1}};\ \dot{m}_{in} = \frac{C_d A_c p_0}{\sqrt{RT_0}}\sqrt{\gamma}\left[\frac{2}{\gamma+1}\right]^{\frac{\gamma+1}{2(\gamma+1)}} \tag{3.25}$$

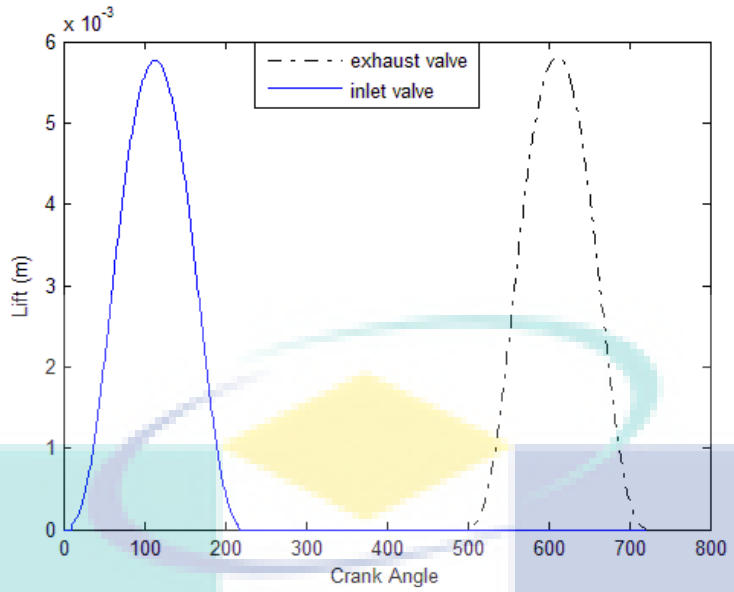

Figure 3.4 Valve lift profile for typical poppet valves with mechanical lifters

While for subsonic flow,

$$\frac{p_T}{p_0} > \left[\frac{2}{\gamma+1}\right]^{\frac{\gamma}{\gamma+1}} \; ; \; \dot{m}_{in} = \frac{C_d A_c p_0}{\sqrt{RT_0}} \left(\frac{p_T}{p_0}\right)^{\frac{1}{\gamma}} \left[\frac{2\gamma}{\gamma-1}\left\{1-\left(\frac{p_T}{p_0}\right)^{\frac{\gamma-1}{\gamma}}\right\}\right]^{\frac{1}{2}} \tag{3.26}$$

where p_T, p_0, T_0 and γ are the downstream static pressure, upstream stagnation pressure, upstream stagnation temperature and ratio of specific heats, respectively. These Eqs., (3.25) and (3.26), are a function of gas properties, valve geometry and thermodynamics states upstream and downstream of the valves. For flow into the combustion chamber, p_0 is the intake port pressure and p_T is the cylinder pressure. On the other hand, p_0 is the cylinder pressure and p_T is the exhaust port pressure for the flow out of the combustion chamber. The value C_d is obtained experimentally from Stiesch [38] and interpolated for the whole valve lift event as shown in Figure 3.5.

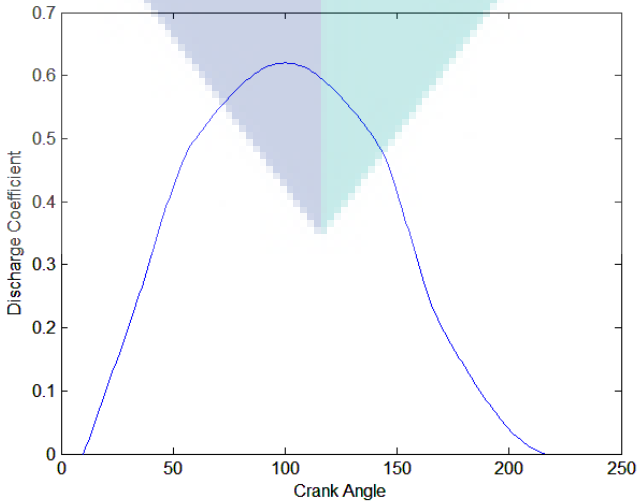

Figure 3.5 Discharge coefficient for one valve event

Once the mass flow rate was determined, it was used in the energy equation and also to obtain the total mass in the combustion chamber. The next section discusses the conservation equations which were used in the zero-dimensional model that is a simplified version of the multi-dimensional model.

3.5 Combustion Process Model

3.5.1 Conservation of Mass

The combustion chamber is assumed to be the control volume of the system, where it has a mass transfer in and out of the system through the intake and exhaust valves. Thus, the mass in the system is defined as Eq. (3.27) [39]

$$\frac{dm}{dt} = \sum_j \dot{m}_j \tag{3.27}$$

where j is the number of flows in ($\dot{m}_j$ positive) or out of the system and m is the total mass in the system.

3.5.2 Conservation of Species

Conservation of species is used to determine the evolution of species inside the combustion chamber due to the chemical reactions. The rate of change of the mass fraction of species i is given by Eq. (3.28) [39]

$$\frac{dY_i}{dt} + \frac{(Y_i - Y_{i_{in}})}{\overline{\rho V}} = \dot{\omega}_i \tag{3.28}$$

where $Y_{i_{in}}$ is the inlet mass fraction and $\dot{\omega}_i$ is the mass reaction rate of the species i.

3.5.3 Conservation of Energy

The first law of thermodynamics equation in differential form is used to model the combustion in the single-zone model. The control volume of the combustion chamber is assumed to be an open thermodynamics system, by ignoring the changes in potential energy. The derivation of the first law of thermodynamics for engine simulations is described extensively by Assanis and Heywood [40]. In differential form, the first law of thermodynamics is expressed as Eq. (3.29)

$$\frac{dU}{dt} = \frac{dQ_h}{dt} - \frac{dW}{dt} + \sum_j \frac{dH_j}{dt} \tag{3.29}$$

where U is the internal energy, Q_h is the heat transfer, W is the work and H_j is the enthalpy of flows entering or leaving the system. By using the definition of each term, Eq. (3.29) then becomes Eq. (3.30)

$$\frac{d(mu)}{dt} = \frac{dQ_h}{dt} - \frac{pdV}{dt} + \sum_j \frac{h_j dm_j}{dt} \tag{3.30}$$

After manipulating Eq. (3.30), the final equation for the temperature change in the single-zone model is given by Eq. (3.31)

$$\frac{dT}{dt} = \frac{1}{C_A}\left[\sum_i\left[\left(\frac{pvR_i}{R} - h_i\right)\frac{dY_i}{dt}\right] - \frac{C_B}{m}\frac{dm}{dt} + \frac{1}{m}\left(\frac{dQ_h}{dt} - \frac{pdV}{dt} + \sum_j \dot{m}_j h_j\right)\right] \tag{3.31}$$

where Q_h is the heat transfer, W is the work and h_j is the enthalpy of flows entering and leaving the system as well as C_A and C_B are defined as

$$C_A = \overline{c_p} - \frac{\rho v}{T} \tag{3.32}$$

$$C_B = h - \rho v \tag{3.33}$$

The derivation of Eq. (3.31) is given in Appendix A.
Once the temperature is obtained, the in-cylinder pressure is determined by using the ideal gas law

$$p = \frac{\rho R_u T}{\overline{W_{mv}}} \tag{3.34}$$

where R_u is the universal gas constant and $\overline{W_{mv}}$ is the mean molecular weight of the mixture.

3.6 Numerical Solutions

A zero-dimensional model solves the first law of thermodynamics equations, as presented in Eq. (3.31). The numerical solution for the temperature change is straightforward because the equation is in the form of a first-order ordinary differential equation. The equation was rearranged so that the change in temperature is on the left hand side. Then, a stiff solver was used to solve Eqs. (3.28) and (3.31) simultaneously. A flow chart of the model is presented in Figure 3.6. The model was coded so that the simulation runs based on the value of crank angle (CA), instead of the pre-defined process with pre-defined combustion, as done by Shaver, Gerdes [41], Canova, Garcin [42] and Killingsworth, Aceves [43]. A pre-defined or segregated process is where the simulation code is divided according to the engine cycle: intake, compression, power and exhaust. Each cycle uses a different set of equations to obtain temperature or pressure change across the CA, which is based on the ideal gas law equation. Then, the ignition occurs based on the pre-defined ignition location with estimated combustion duration, where the ignition delay has been measured according to the experiment. There is no detailed chemical reaction involved. For the simulation based on the value of CA, it uses the energy equation for the entire engine cycle to solve the temperature change in the chamber with detailed chemical reactions involved. This method gives an advantage in predicting the chemical reaction behavior along the CA step, because the chemical reactions fully control the HCCI engines. At the beginning of the simulation, the engine parameters and initial operating condition were defined, which were based on the experimental data [44, 45]. Then, the mixture composition in the combustion chamber and inlet manifold was initialized. It was assumed that the initial composition in the combustion chamber before IVO consists of only air and a mixture of air and fuel is introduced after the IVO.

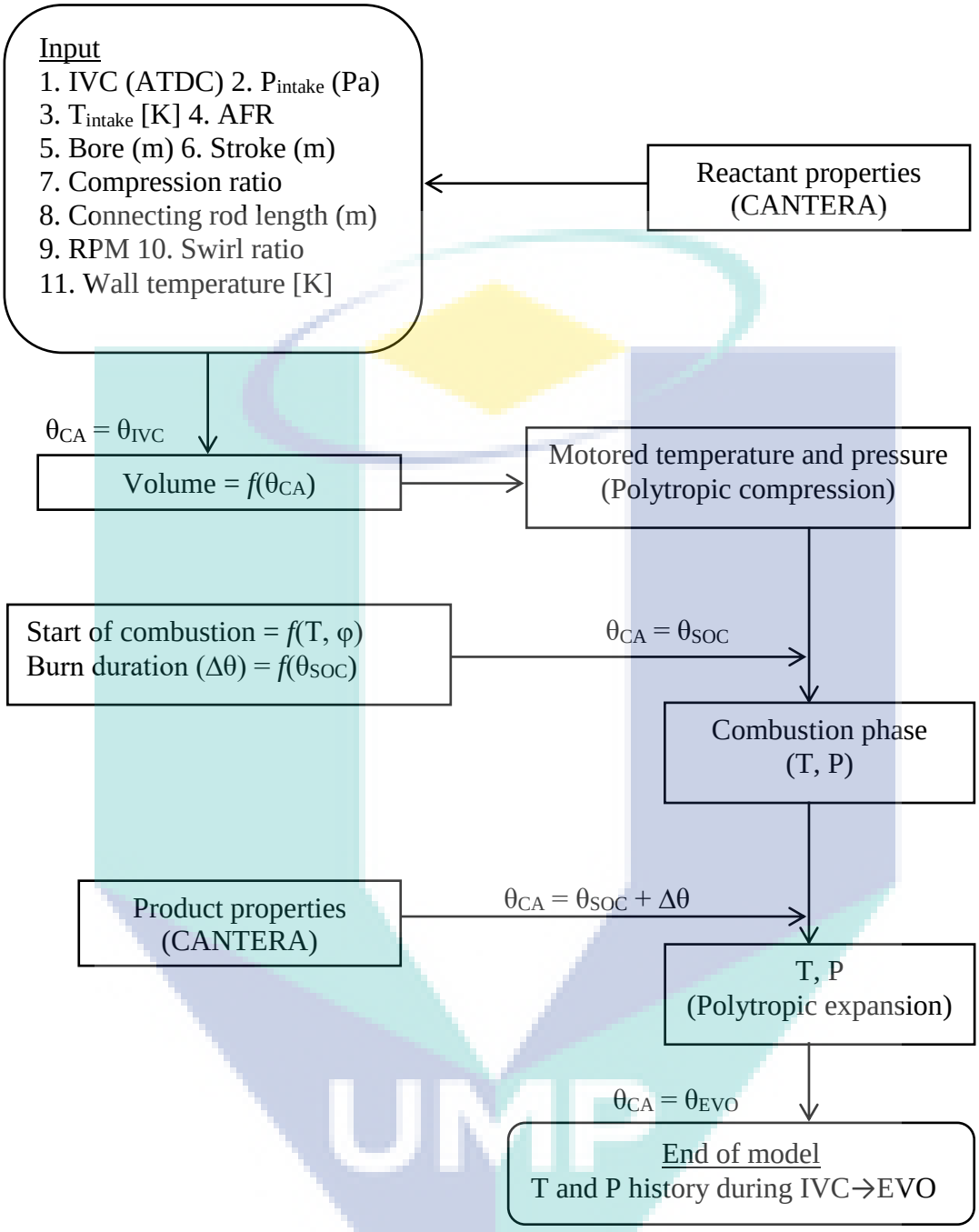

Figure 3.6. An algorithm flow chart for zero-dimensional single-zone model simulation.

A typical valve profile was determined based on Eq. (3.18), which was used to represent the valve motion and also to get the inlet mass flow rate ($\dot{m}_{in}$). The simulation began from 0°CA, where the piston was at TDC, and finished at EVO. The entire simulation consists of three parts: before IVO, before IVC and before EVO, as shown in Figure 3.6. For the first part, the piston was in downward motion and the air was expanded before being mixed with the intake mixture. Once the intake valve was opened (second part), the air in the combustion chamber was mixed with the intake mixture. In this process, the mass was added to the combustion chamber based on Eq. (3.27). The cylinder volume was expanding and it is expected that the mixture temperature was decreasing at this stage. The final part is where the main combustion occurred, which was after IVC and before EVO. At this stage, the piston was in

upward motion after IVC, compressing the gas mixture. The chemical kinetics plays an important role as it determines the start of combustion. Once the piston passes the TDC mark, it is in downward motion again, expanding the mixture and the simulation stops at EVO. The simulation solves the energy and species equations for the entire process. Therefore, this technique has eliminated the segregated process as usually done in zero-dimensional modeling. Segregated process is where the simulation is divided into four parts in one engine cycle: intake, compression, expansion and exhaust. Thus, the simulation uses four different sets of equations to cater for each process. In this study, the simulation uses only one set of equations for all the processes. This ensures the in-cylinder properties are consistent from one process to another. Cantera is an open source software package for chemical kinetics mechanism and is widely used [46]. New researchers could easily adopt Cantera for their research needs given the software's capability to integrate with MATLAB, FORTRAN and Python languages. The chemical kinetics mechanism files can be obtained in Chemkin format, where the file is then be converted to a Cantera-readable file. The use of a chemical reaction mechanism enables the study of the chemical species interaction, where the interaction is influenced by the temperature, pressure and species mass fraction. Furthermore, the chemical reaction mechanism would be able to give a better understanding in the combustion study. The base code used in this study for zero-dimensional single zone engine model written in MATLAB and using Cantera for the chemical kinetics calculations is included.

4. RESULTS AND DISCUSSION

The validation of the zero-dimensional single zone model against the experimental results from the literature will be presented in this chapter. Two experimental data sets were used for validation purpose: one is the HCCI engine fuelled with diesel [44] and the other with gasoline [45]. This Chapter also presents the results of numerical modeling. The engine conditions including intake temperature, intake pressure, engine speed and the compression ratio will be varied to analyse the ability of the model to predict the combustion, performance and emissions characteristics of HCCI engines. The numerical results will be compared with experimental results from CI and SI engines to understand the advantages of HCCI engines over CI and SI engines. The use of fuel blends is an important concept for the HCCI engine. It helps to study the ability of HCCI engines to use a variety of fuels. This Chapter will describe the performance and emissions characteristics of HCCI engines and compare the results with CI and SI engines first. Then the effect of engine parameters on combustion and performance characteristics of both diesel and gasoline HCCI engines will be presented. After that, the effects of fuel blends in HCCI engines will be described. The summary will conclude the Chapter.

4.1.1 Model Validation of Diesel HCCI

In this section, the simulation models were validated by the experimental results that were conducted by Guo, Neill [44] on a four stroke single cylinder diesel engine which was modified for HCCI operation at a fixed engine speed of 900 rpm under the full engine load condition for diesel fuel. The detail specifications of the engines are presented in Table 4.1. The schematic diagram of the engine setup is presented in Figure 4.1.

Table 4.1 Engine model specifications (Guo, Neill [44])

Engine parameters	Value
Type	4 stroke, single cylinder
Bore (mm)	82.55
Stroke (mm)	114.3
Displacement (L)	0.6117
No. of cylinders	1
Compression ratio	4.6-16
Connecting rod length (mm)	254
Combustion chamber	Pancake shape
Intake Valve Close (°CA)	-144
Exhaust Valve Open (°CA)	140
Fuel system	Air-assist port fuel injection

The engine was modified from the standard ASTM guideline by the addition of an air-assist port fuel injection system and other hardware and software needed for the control of critical engine parameters such as intake air temperature, air/fuel ratio, exhaust gas recirculation and intake and exhaust back pressure. A port fuel injector for flexible fuel vehicles was modified to provide air-assist atomization of liquid fuels. Surge tanks were installed in the intake and exhaust systems to minimize pressure pulsations of the intake and exhaust gasses, thereby improving engine operational stability and airflow measurement. The low-speed data acquisition system

is based on National Instruments' PXI hardware platform. The hardware is controlled by data acquisition and control software (Sakor Technologies, Inc., DynoLAB™ PT), which provided stable control of the engine speed and load conditions, as well as critical parameters such as engine coolant and lubricating oil temperatures, intake air pressure and temperature, exhaust back pressure, fuel injection timing, and the quantity of fuel injected. The engine was coupled to an eddy current dynamometer that absorbed engine load. A variable-speed ac motor, coupled to the dynamometer with an overdrive clutch, was used to start and motor the engine before stable HCCI combustion was initiated, as well as to maintain engine speed when HCCI combustion was unstable. In this study, the initial conditions for the intake pressure and temperature were set as P_{intake}=100 kPa and T_{intake}=333 K. The intake air temperature was set 20K higher than the actual temperature to account for the mixing effects [44]. A different study also stated that the intake temperature for a single-zone model has to be increased up to 30K, while up to about 10K for a multi-zone model [47]. The assumption of uniform wall temperature for the entire engine cycle, uniform in-cylinder temperature and pressure, and a potential limitation of the chemical chemistry as well may contribute to the adjustment of the intake temperature [44]. The wall temperature (T_{wall}) was set to be 530K for a CI engine [48]. However, the wall temperature used in the numerical studies varies from one engine to another [48-50], where the wall temperature ranges from 293K [51] to approximately 800K [49]. The exhaust temperature and pressure were approximated at 1000K and 101.3kPa, respectively [36], where the approximated value is close to measurement of a diesel engine [52]. At the beginning of the simulation, where CA is less than IVO, the mixture composition in the chamber was assumed to be only air with no fuel. The fuel is being introduced into the chamber during the IVO period, where the fuel quantity is based on the air-fuel ratio used in the experiment.

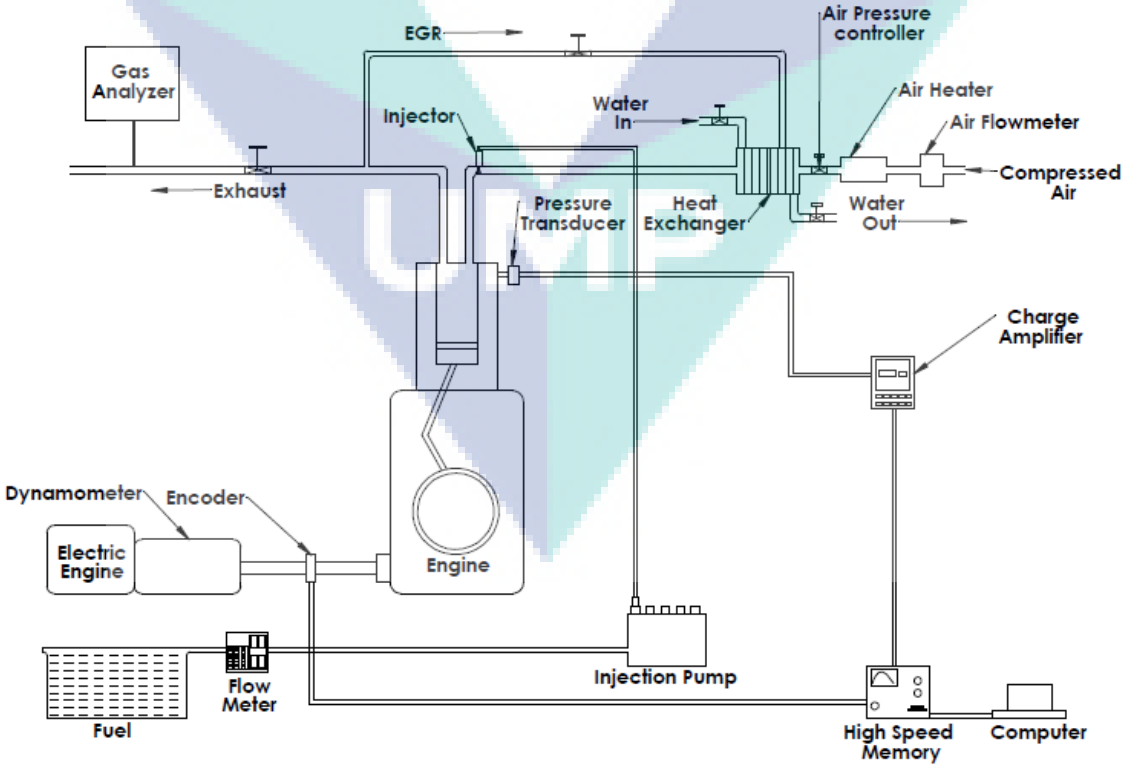

Figure 4.1 Schematic diagram of the HCCI engine set up, reproduced from [44]

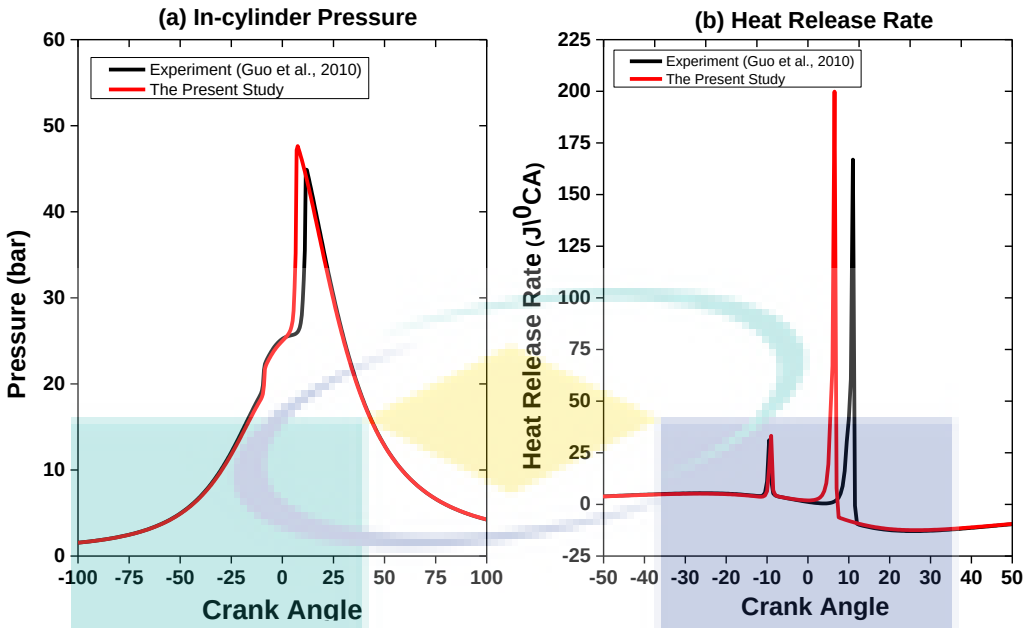

Figure 4.2 Comparison between zero-dimensional single zone model with experimental data [44]. CR=10, N=900 rpm, T_{in}=333 K, P_{in}=100 kPa, AFR=50

To further validate the applicability of the developed reaction mechanism for engine simulations, numerical simulations were performed and compared against the HCCI engine experiments. The obtained results show good agreement with the experimental published results and capture important combustion phase trends as engine parameters are varied with a maximum percentage of error which is less than 6%. As presented in Figure 4.2, the numerical simulation was able to capture elements of HCCI combustion of diesel, particularly the low-temperature reaction (LTR). Figure 4.2(a) plots the in-cylinder pressure and Figure 4.2(b) plots the heat release rate obtained from experiments done by [44] and the present study, at a fixed engine speed of 900 rpm under constant intake temperature of 333 K and air-fuel ratio of 50 conditions. As can be seen, the peak cylinder pressure is adequately reproduced, indicating that the important reaction pathways are very well represented. In comparison, the main combustion stage (MCS) predicted by the numerical simulation is advanced compared to the experimental results as presented in Figure 4.2(b). A spike in the predicted heat release rate was observed during the MCS. This spike was caused by the rapid oxidation of all CO accumulated to this point in the simulation to CO_2 [53]. The conversion of CO to CO_2 is predicted to happen rapidly once the required temperature is reached because only a few reactions are involved. Rapid oxidation of CO to CO_2 has not been observed experimentally or reported in this study. The assumption of uniform mixture temperature and mixture composition contributes to this overly-rapid heat release rate.

4.1.2 Gasoline HCCI

In this section, the simulation models were validated by the experimental results that were conducted on a four stroke inline-4 cylinders gasoline engine which was modified for HCCI operation at a fixed engine speed of 1500 rpm under the full engine load condition for gasoline fuel surrogate. The detail specifications of the engines are presented in Table 4.2 [45]. The schematic diagram of the engine setup is presented in Figure 4.3.

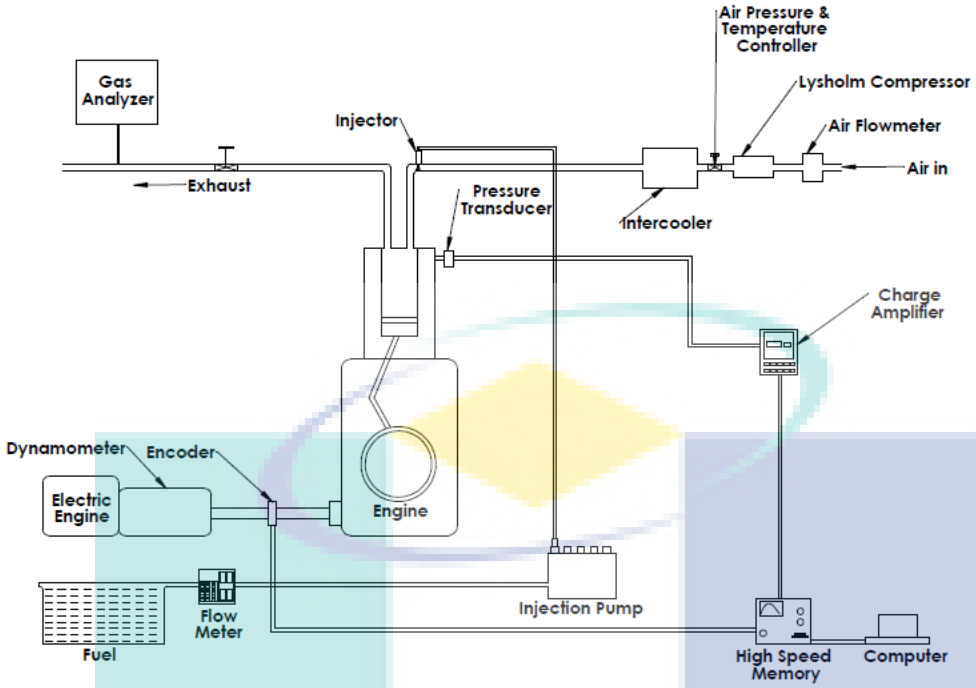

Figure 4.3 Schematic diagram of the HCCI engine set up, reproduced from [45].

The engine was modified from the standard setup by the addition of hardware and software needed for the control of critical engine parameters such as intake air temperature, air-fuel ratio, exhaust gas recirculation and intake and exhaust back pressure. The intake mean pressure was adjusted by varying the motor drive speed. The intake gas temperature was adjusted by a water-cooled intercooler. The partition ratio of a three-way valve was controlled to realize given intake temperature. The mean pressure in the exhaust pipe was controlled using an exhaust throttle valve. The cylinder pressure of the cylinder was measured by a piezoelectric pressure transducer (Kistler 6052c, 6117b). The crank angle of the 50% burn (CA50) was used to monitor the combustion phasing, and grossIMEP was used to recognize the output power of an individual cylinder. To balance the cylinder-to-cylinder variation of CA50 and grossIMEP, the amount of supplied fuel for the each cylinder were adjusted. All of the pressure analysis data including apparent HRR, mean effective pressures and pressure rise rate were computed from the ensemble-averaged pressure trace taken over 100 cycles. Piezo-resistive pressure transducers (Kistler 4005B) were mounted on the intake and the exhaust manifolds for the measurements of intake and exhaust pressure pulsations. In this study, the initial conditions for the intake pressure and temperature were set as P_{intake}=100 kPa and T_{intake}=393 K. The intake temperature for the zero-dimensional model was set 15°C higher than the actual to account for the mixing effects. This is consistent with Bunting, Eaton [47] and Guo, Neill [44], where the intake temperature for the zero-dimensional model was set 10 – 30 K higher than the actual. The wall temperature (T_{wall}) was set to be 353K which is consistent with Barroso, Escher [51] and Su, Mosbach [54]. However, the wall temperature used in the numerical studies varies from one engine to another [48-50], where the wall temperature ranges from 293K [51] to approximately 800K [49]. The exhaust temperature and pressure were approximated at 700K and 101.3kPa, respectively [36], where the approximated value is close to measurement of a gasoline engine [52]. At the beginning of the simulation, which is before the IVO, the mixture in the chamber was assumed to be only air and the fuel-air mixture was added according to the pre-set air-fuel ratio value after the IVO.

Table 4.2. Engine model specifications (Gotoh, Kuboyama [45])

Engine parameters	Value
Type	4 stroke, Inline-4 cylinder
Bore (mm)	86
Stroke (mm)	86
Displacement (L)	0.5
No. of cylinders	4
Compression ratio	12
Connecting rod length (mm)	200
Fuel	Gasoline (RON 91)
Intake Valve Close (°CA)	-180
Exhaust Valve Open (°CA)	156
Fuel system	Air-assist port fuel injection

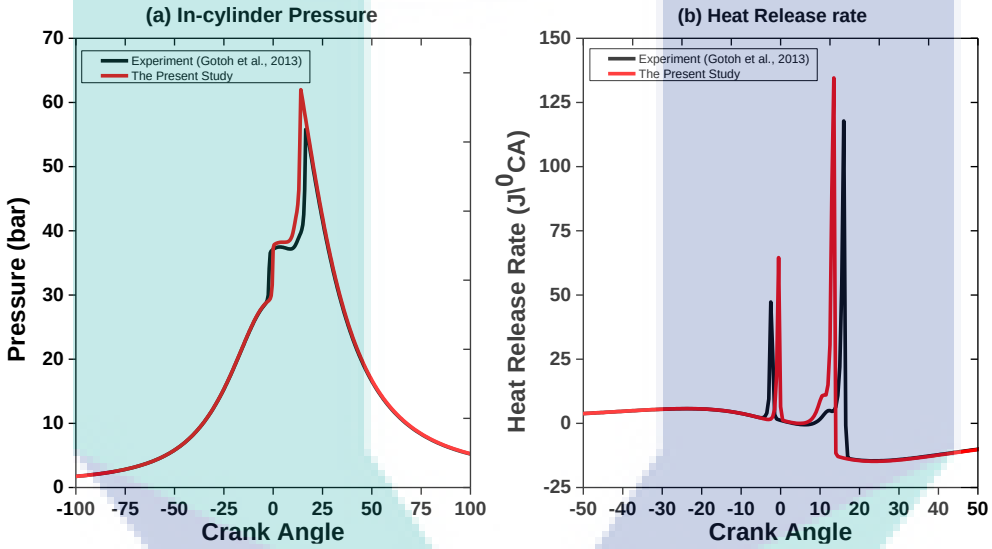

Figure 4.4 Comparison between zero-dimensional single zone model with experimental data [45]. CR=12, N=1500 rpm, T_{in}=393 K, P_{in}=100 kPa, AFR=40

To further validate the applicability of the developed reaction mechanism for engine simulations, numerical simulations were performed and compared against the HCCI engine experiments. The obtained results show good agreement with the experimental published results and capture important combustion phase trends as engine parameters are varied with a maximum percentage of error which is less than 4%. As presented in Figure 4.4, the numerical simulation was able to capture elements of HCCI combustion of gasoline surrogate fuel, particularly the LTR. Figure 4.4(a) plots the in-cylinder pressure and Figure 4.4(b) plots the heat release rate obtained from experiments done by Gotoh, Kuboyama [45] and the present study, at a fixed engine speed of 1500 rpm under constant intake temperature of 393 K and air-fuel ratio of 40 conditions. As can be seen, the peak cylinder pressure is predicted higher than the experiment. The predicted maximum in-cylinder pressure is evidently slightly higher than that of the experiment due to the limitation of the zero-dimensional model, where the entire combustion chamber is assumed to be homogenous. In comparison, MCS predicted by the numerical simulation is advanced compared to the experimental data as presented in Figure 4.4(b). A spike in the predicted heat release rate was observed during the MCS. This spike was caused by the rapid oxidation of all CO accumulated to this point in the simulation to CO_2. The conversion of CO to CO_2 is predicted to happen rapidly once the required temperature

is reached because only a few reactions are involved. The assumption of uniform mixture temperature and mixture composition contributes to this overly-rapid heat release rate. Overall, the combustion phasing is in good agreement with the experimental data, demonstrating that the zero-dimensional single-zone model can be used in HCCI engine simulations.

4.2 Influence of Engine Parameters

In this section, the effect of engine speed, intake air temperature, intake air pressure and compression ratio on combustion and performance characteristics of HCCI engine is investigated using numerical simulations for both diesel HCCI and gasoline HCCI. The engine specifications and fuels used for validation purposes were also used here to investigate the effects of engine parameters.

4.2.1 Diesel HCCI

Engine speed is an important parameter which has a significant effect on combustion and performance of HCCI engines. Figure 4.5 illustrates the effect of engine speed on diesel HCCI combustion and performance for a constant intake temperature of 333 K. Engine speed was varied from 600 rpm to 1200 rpm. From the Figure 4.5(a) it is clearly seen that in-cylinder pressure increases with increasing engine speed up to 900 rpm and then decreases with further increasing engine speed. The most important reason is heat loss through the cylinder wall during the compression stroke. With the engine speed increasing, the accumulated heat loss during the compression stroke reduced significantly because of the shorter cyclic period, which increases the in-cylinder temperature at the end of the compression stroke. Therefore, the chamber could achieve a higher maximum pressure at higher engine speed due to less heat loss through the cylinder wall [55]. In addition, peak pressure location is retarded with the increase of engine speed. This is due to a significantly retarded MCS, as presented in Figure 4.5(b). The heat release rate during the MCS is also reduced with retarded combustion due to the increasing combustion chamber volume after top dead center. This leads to lower combustion chamber temperatures and a corresponding decrease in the oxidation reaction rates [56]. However, the effect of engine speed on the LTR phase tends to be relatively weak, reflecting its strong dependence on temperature history [57]. To observe the influence of engine speed on the performance of HCCI engines, five typical speeds were selected for the simulation. As are presented in Figures 4.5(d)-(f), IMEP, IT and IP increase with increasing engine speed up to 900 rpm and then decreases with further increasing engine speed. Maximum IMEP, IT and IP were obtained as 5.69 bar, 27.72 Nm and 2.61 kW. At higher engine speed the performance was less. This is because of that, with the increase of engine speed, the combustion duration is shortened with respect to time and affects the performance of HCCI engines [58]. Moreover, volumetric efficiency depends on engine speed. Because of the changing volumetric efficiency and increased friction forces at higher engine speed, the IMEP, IT and IP were less[59].

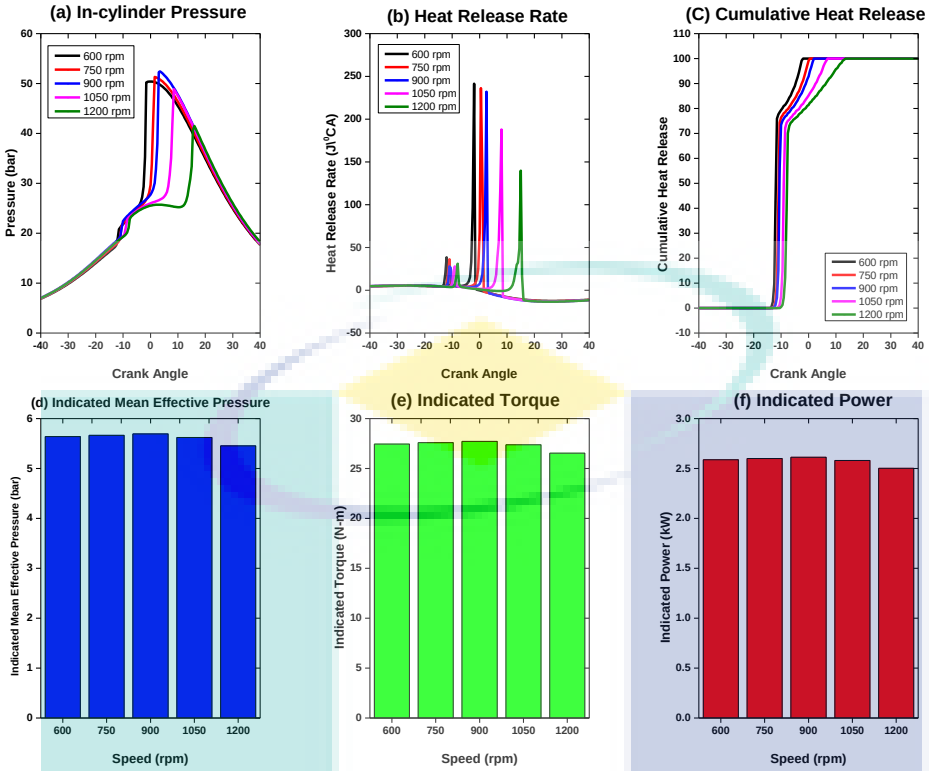

Figure 4.5 Influence of speed on combustion and performance characteristics in HCCI engine. CR=10.0, T_{in}=333 K, P_{in}=100 kPa, AFR=50

Intake air temperature is the most critical and widely used engine operation parameter to control the phasing of HCCI combustion. Figure 4.6 illustrates the effect of intake temperature on HCCI combustion and performance for a constant AFR of 50. Intake temperature of the air was varied from 333 K to 393 K. Stable HCCI combustion was obtained for a wide range of temperatures. As presented in Figure 4.6(a) the auto-ignition timing was advanced with the increase of intake air temperature. The phasing of both LTR and MCS were advanced. Furthermore, it can also be clearly seen from Figure 4.6(b) that rapid heat release rate occurs due to higher pressure rise rate. Thus, HCCI combustion deteriorated due to knocking and cylinder pressure decreased with the increase of inlet air temperature. The LTR heat release profiles were found to be quite similar, although they were advanced as temperature increased. However, increasing the intake temperature significantly enhances the heat release rate of the MCS. The increasingly advanced phasing of the MCS contributes to the increased heat release rate [60]. To investigate the influence of intake air temperature on the performance of HCCI engines, five typical temperatures were selected for the simulation. As are presented in Figures 4.6(d)-(f) IMEP, IT and IP decrease with increasing intake temperature. This is because there are key chemical reactions in the low-temperature phase. These reactions depend on the system temperature and AFR. $C_7H_{15}O_2$=$C_7H_{14}OOH$ is the most important reaction in low-temperature phase. $C_7H_{14}OOH$ retards the process of low-temperature oxidation, and it plays the most important role in the occurrence of the negative temperature coefficient (NTC) phase [57, 61]. Under the specific operating condition, the maximum IMEP, IT, and IP occur when intake temperature is 360 K. Obviously, the intake temperature is very critical, i.e., a small change of intake temperature leads to large variations in the performance of HCCI.

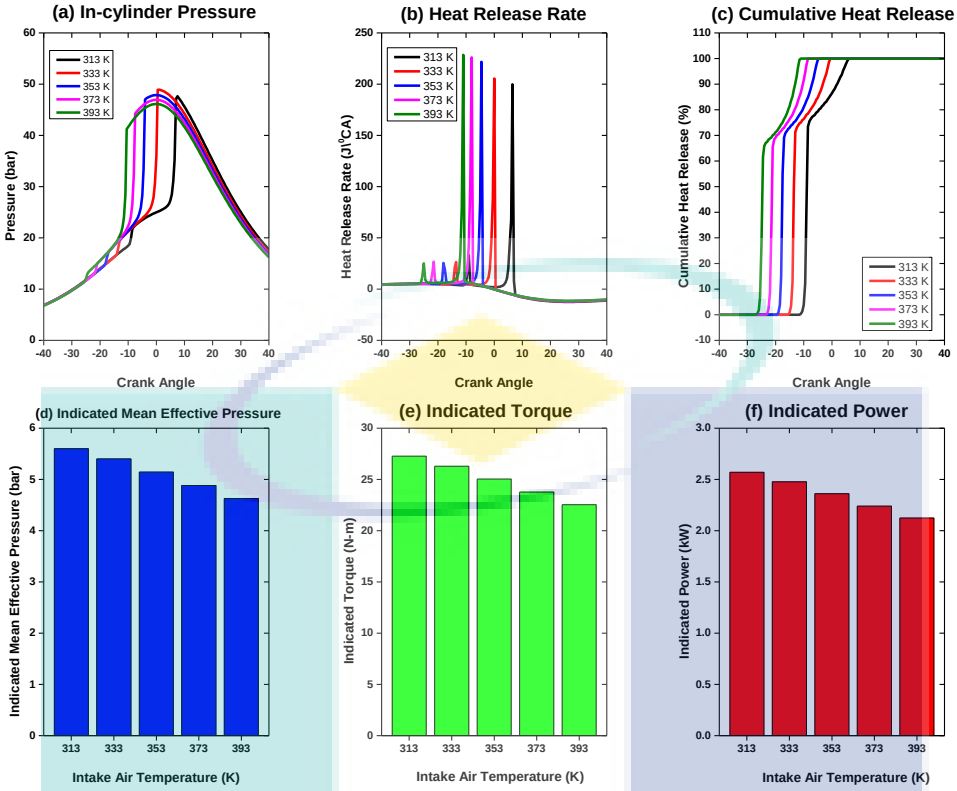

Figure 4.6 Influence of intake air temperature on combustion and performance characteristics in the HCCI engine. CR=10.0, N=900 rpm, P_{in}=100 kPa, AFR=50

Intake air pressure boosting has a significant effect on the combustion and performance of HCCI engines as well as is a common way to improve power output. In this study, the effect of boosting on HCCI combustion and performance was examined at a constant AFR and intake air temperature condition. As presented in Figure 4.7(a), boosting the intake pressure tends to significantly increase the peak cylinder pressure during the compression stroke. The reason is that the collision frequency among molecules increases with the increase of the boost pressure, which leads to the increase of the combustion reaction velocity [62]. Since the quantity of fuel injected is increased as intake pressure increases to maintain a constant AFR, the LTR stage is advanced and intensified. This leads to a shorter NTC delay period and significantly advances phasing of the MCS, as presented in Figure 4.7(b). The reason for this is the combustion reaction velocity which increases with the increasing boost pressure [63, 64]. To investigate the influence of intake air pressure on the performance of HCCI engines, five typical pressures ranging from 100 kPa to 200kPa were selected for the simulation. As are presented in Figures 4.7(d)-(f) IMEP, IT and IP increases with increasing intake air pressure. The maximum IMEP, IT, and IP were obtained at 200 kPa. The use of a higher inlet pressure can bring in more air, which leads to an increase of the amount of fuel that can be injected and an increase of the maximum IMEP, IT and IP those can be achieved. On the other hand, the engine can operate stably at a leaner air fuel ratio with an increasing inlet pressure, which leads to lower values of IMEP, IT and IP. However, the benefits of intake boost would have been much greater if the combustion phasing had been controlled independently using different intake temperature, EGR, or other methods. The results indicate that an increase in the boost pressure causes the need of leaner mixture, and requires more advanced injection timing to achieve the maximum engine torque [65, 66].

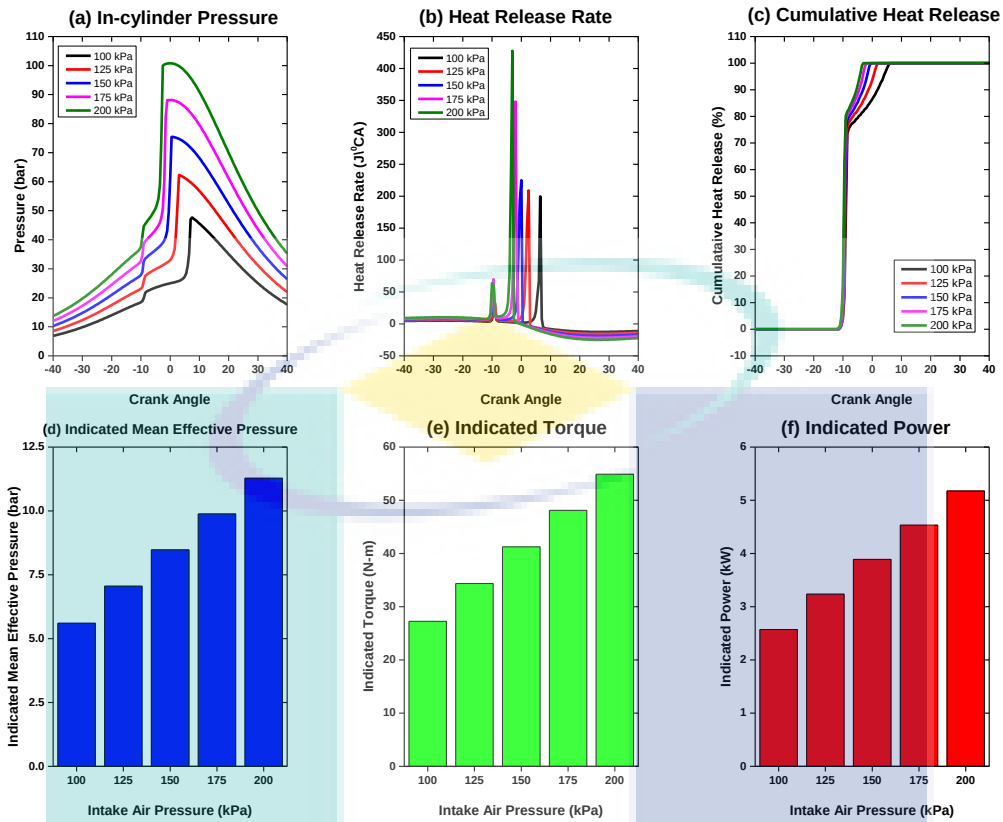

Figure 4.7 Influence of intake air pressure on combustion and performance characteristics in the HCCI engine. CR=10.0, N=900 rpm, T_{in}=333 K, AFR=50

The compression ratio is another important engine parameter which also has a significant effect on combustion and performance characteristics of HCCI engines. Figure 4.8 presents that increasing the compression ratio advances the combustion process and increases the peak cylinder pressures. This is primarily due to the effect of increased compression temperatures and pressures as the compression ratio increases, which enhances diesel oxidation. As presented in Figure 4.8(b), the phasing of both LTR and MCS phases were advanced with increasing compression ratio [67]. To investigate the influence of compression ratio on the performance of HCCI engines, five typical compression ratios were selected for the simulation. As are presented in Figures 4.8(d)-(f) IMEP, IT and IP increases with increasing compression ratio. This is because there are key chemical reactions which occur during the compression stroke. These reactions depend on the in-cylinder pressure and temperature. Due to increasing compression ratio oxidation of diesel is enhanced which ultimately help to increase IMEP, IT and IP [61]. Under the specific operating condition, the maximum IMEP, IT, and IP occur when the compression ratio is 16. It is obvious that the compression ratio is very critical, i.e., a small change of compression ratio leads to large variations in the performance of HCCI.

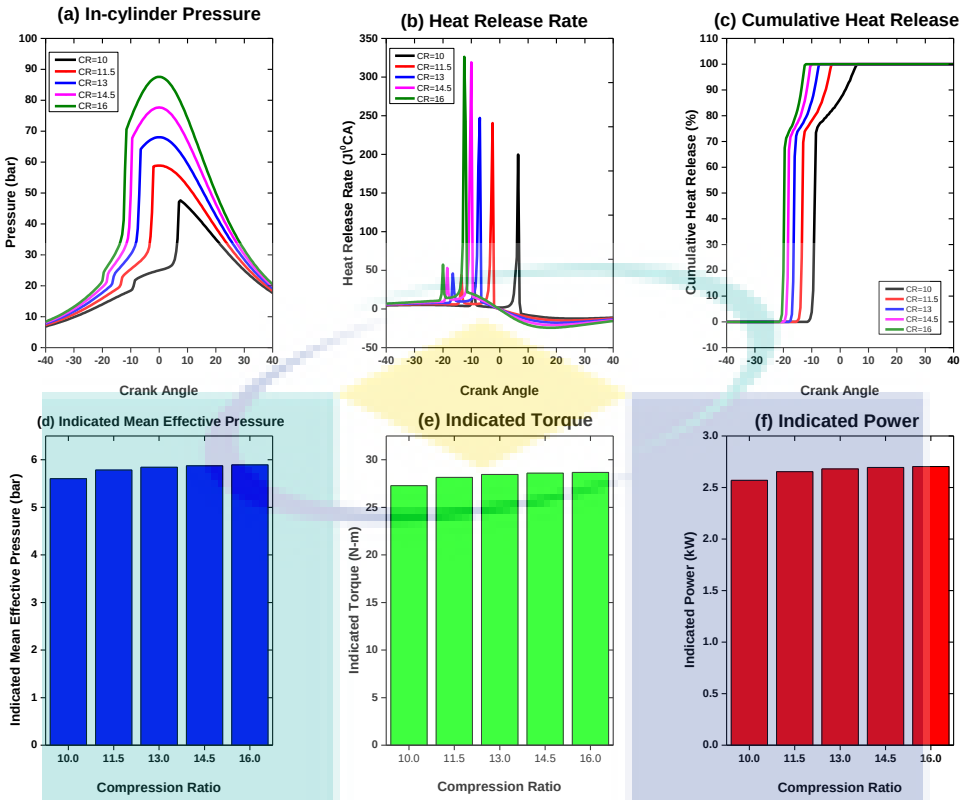

Figure 4.8 Influence of Compression Ratio on combustion and performance characteristics in the HCCI engine. N=900 rpm, T_{in}=333 K, P_{in}=100 kPa, AFR=50.

4.2.2 Gasoline HCCI

Engine speed is an important parameter which has a significant effect on combustion and performance of HCCI engines. Figure 4.9 illustrates the effect of engine speed on HCCI combustion and performance for a constant intake temperature of 393 K. Engine speed was varied from 600 rpm to 1800 rpm. From Figure 4.9(a) it is clearly seen that in-cylinder pressure increases with increasing engine speed up to 1500 rpm and then decreases with further increasing engine speed. Peak pressure location is retarded with the increase of engine speed. This is due to a significantly retarded MCS, as presented in Figure 4.9(b). The heat release rate during the MCS is also reduced with retarded combustion due to the increasing combustion chamber volume after top dead center. This leads to lower combustion chamber temperatures and a corresponding decrease in the oxidation reaction rates. However, the effect of engine speed on the LTR phase tends to be relatively weak, reflecting its strong dependence on temperature history [57]. To observe the influence of engine speed on the performance of HCCI engines, five typical speeds were selected for the simulation. As are presented in Figures 4.9(d-f), IMEP, IT and IP increases with increasing engine speed up to 1500 rpm and then decreases with further increasing engine speed. This is because of that, with the increase of engine speed, the combustion duration is shortened with respect to time and affects the performance of HCCI engines [58].

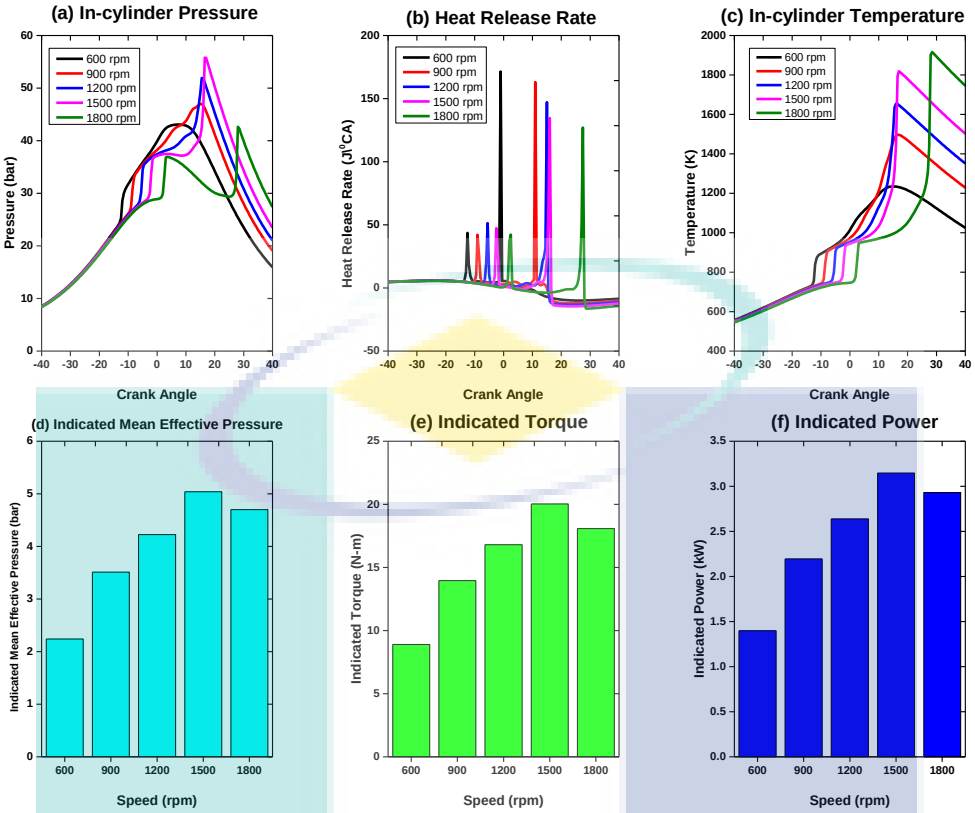

Figure 4.9 Influence of speed on combustion and performance characteristics in the HCCI engine. CR=12.0, T_{in}=393 K, P_{in}=100 kPa, AFR=40

Intake air temperature is the most critical and widely used engine operation parameter to control the phasing of HCCI combustion. Figure 4.10 illustrates the effect of intake temperature on HCCI combustion and performance for a constant AFR of 40. Intake temperature of the air was varied from 373 K to 453 K. Stable HCCI combustion was obtained for a wide range of temperatures. As presented in Figure 4.10(a) the auto-ignition timing was advanced with the increase of intake air temperature. The phasing of both LTR and MCS were advanced. Furthermore, it can also be clearly seen from Figure 4.10(b) that the rapid heat release rate occurs due to higher pressure rise rate. Thus, HCCI combustion deteriorated due to knocking and cylinder pressure decreased with the increase of inlet air temperature. The LTR heat release profiles were found to be quite similar, although they were advanced as temperature increased. However, increasing the intake temperature significantly enhances the heat release rate of the MCS. The increasingly advanced phasing of the MCS contributes to the increased heat release rate [60]. To investigate the influence of intake air temperature on the performance of HCCI engines, five typical temperatures were selected for the simulation. As are presented in Figures 4.10(d-f), IMEP, IT and IP decrease with increasing intake temperature. This is because there are key chemical reactions in the low-temperature phase. These reactions depend on the system temperature and AFR. $C_7H_{15}O2=C_7H_{14}OOH$ is the most important reaction in the low-temperature phase. $C_7H_{14}OOH$ retards the process of low-temperature oxidation, and it plays the most important role in the occurrence of the negative temperature coefficient (NTC) phase [57, 61]. Under the specific operating condition, the maximum IMEP, IT, and IP occur when intake temperature is 373 K. Obviously, the intake temperature is very critical, i.e., a small change of intake temperature leads to large variations in the performance of HCCI.

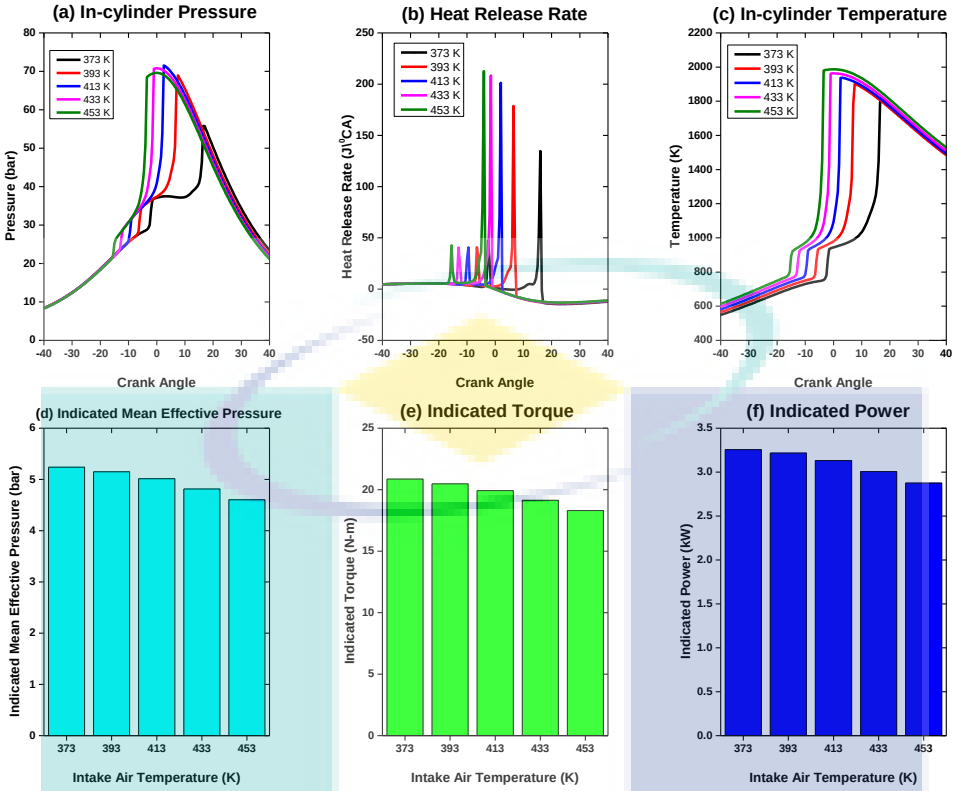

Figure 4.10 Influence of intake air temperature on combustion and performance characteristics in the HCCI engine. CR=12.0, N=1500 rpm, P_{in}=100 kPa, AFR=40

Intake air pressure boosting has a significant effect on the combustion and performance of HCCI engines as well as is a common way to improve power output. In this study, the effect of boosting on HCCI combustion and performance was examined at a constant AFR and intake air condition. As presented in Figure 4.11(a), boosting the intake pressure tends to significantly increase the cylinder pressure during the compression stroke. Since the quantity of fuel injected is increased as intake pressure increases to maintain a constant AFR, the LTR stage is advanced and intensified. This leads to a shorter NTC delay period and significantly advances phasing of the MCS, as presented in Figure 4.11(b). The reason for this is the combustion reaction velocity which increases with the increasing boost pressure [63, 64]. To investigate the influence of intake air pressure on the performance of HCCI engines, five typical pressures ranging from 100 kPa to 200kPa were selected for the simulation. As are presented in Figures 4.11(d-f), IMEP, IT and IP increase with increasing intake air pressure. The maximum IMEP, IT, and IP were obtained at 200 kPa. The results indicate that an increase in the boost pressure causes the need for leaner mixture, and requires more advanced injection timing to achieve the maximum engine torque [65, 66].

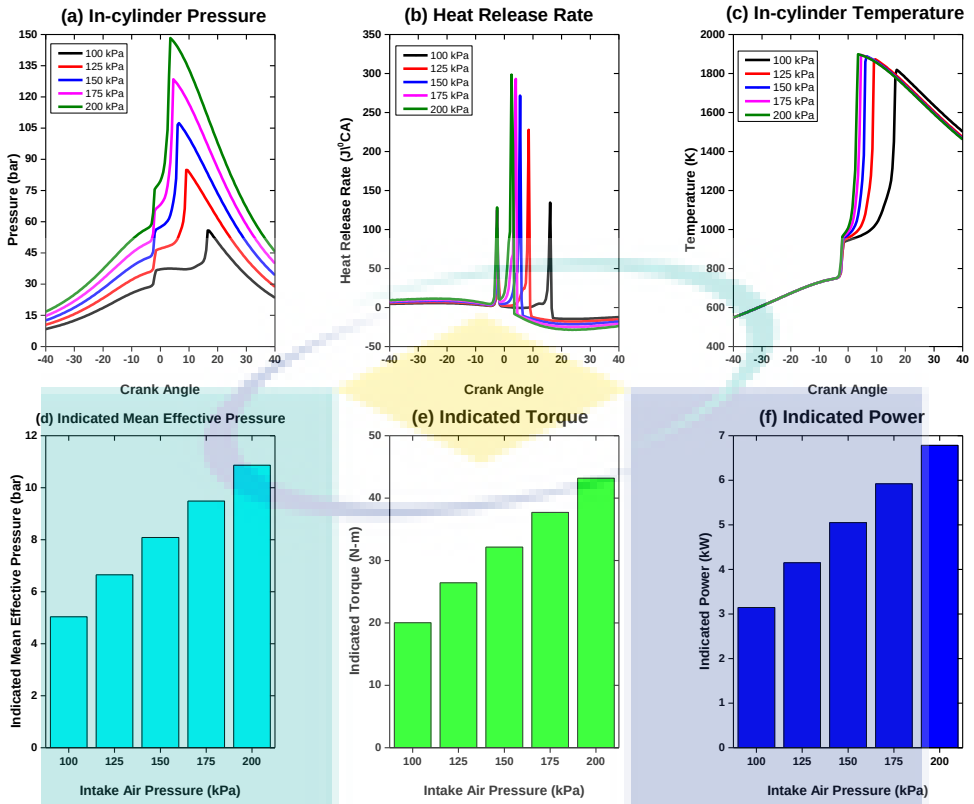

Figure 4.11 Influence of intake air pressure on combustion and performance characteristics in the HCCI engine. CR=12.0, N=1500 rpm, T_{in}=393 K, AFR=40.

The compression ratio is another important engine parameter which also has a significant effect on combustion and performance characteristics of HCCI engines. Figure 4.12 presents that increasing the compression ratio advances the combustion process and increases the peak cylinder pressures. This is primarily due to the effect of increased compression temperatures and pressures as the compression ratio increases, which enhances gasoline surrogate fuel oxidation. As presented in Figure 4.12(b), the phasing of both LTR and MCS phases were advanced with increasing compression ratio [67]. To investigate the influence of compression ratio on the performance of HCCI engines, five typical compression ratios were selected for the simulation. As are presented in Figures 4.12(d-f), IMEP, IT and IP increase with increasing compression ratio. This is because there are key chemical reactions which occur during the compression stroke. These reactions depend on the in-cylinder pressure and temperature. Due to increasing compression ratio oxidation of gasoline surrogate fuel is enhanced which ultimately help to increase IMEP, IT and IP [61]. Under the specific operating condition, the maximum IMEP, IT, and IP occur when the compression ratio is 16. It is obvious that the compression ratio is very critical, i.e., a small change of compression ratio leads to large variations in performance of HCCI.

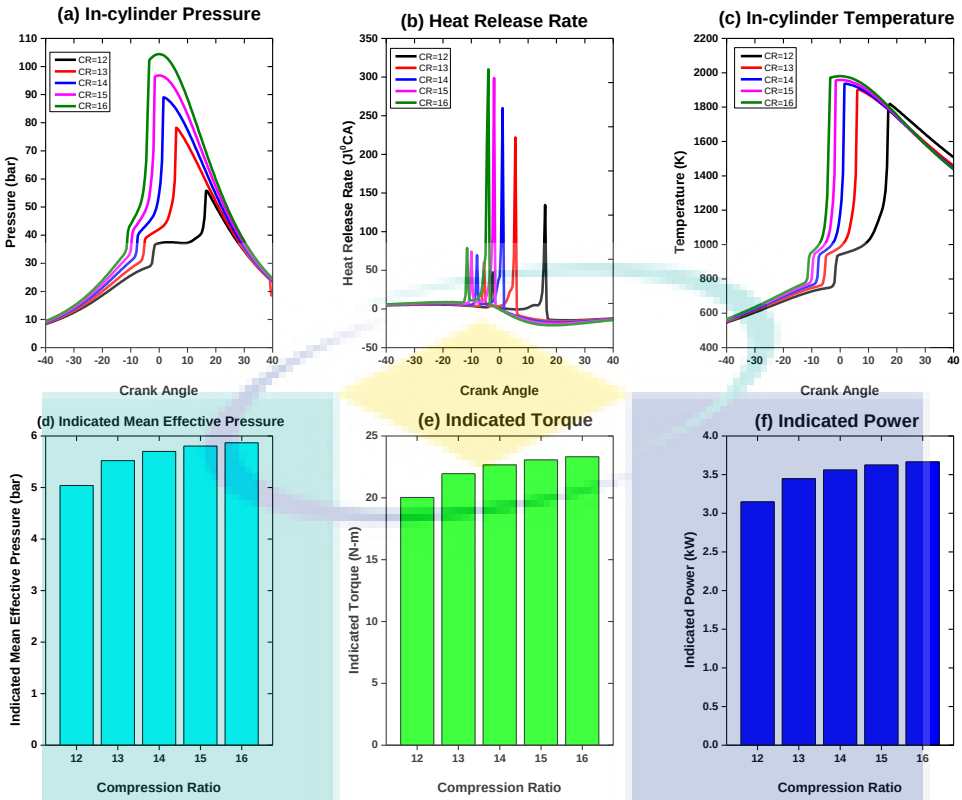

Figure 4.12 Influence of Compression Ratio on combustion and performance characteristics in the HCCI engine. N=1500 rpm, T_{in}=393 K, P_{in}=100 kPa, AFR=40

4.3 Different Fueled HCCI

Intake temperature plays an important role in HCCI combustion because HCCI combustion depends on the chemical kinetics. Charge mixture is compressed until autoignition temperature reaches [36, 68]. In addition, suitable fuel should be selected avoiding misfire and knocking. In this way, alcohols resist to not only knocking combustion but also reducing the harmful exhaust emissions in HCCI combustion [69]. As an alternative fuel, alcohol seems to be the most promising choices among other fuels in order to control HCCI combustion. In this study, the effects of pure n-heptane, and ethanol/n-heptane mixtures and butanol/n-heptane mixtures were investigated on HCCI combustion, performance and emissions using numerical simulations. N-heptane percentages used in the ethanol and butanol mixtures were chosen 70% and 85% by volume where E15 contains 85% n-heptane and 15% ethanol; E30 contains 70% n-heptane and 30% ethanol; Bu15 contains 85% n-heptane and 15% butanol as well as Bu30 contains 70% n-heptane and 30% butanol. A numerical study was performed at 900 rpm engine speed and constant lambda (λ= 2) at different intake temperatures of 313 K, 333 K, 353 K, 373 K and 393 K in order to observe the controlling of HCCI combustion. The reason of selecting this range of intake temperatures is that lower intake air temperature cannot achieve the test fuels' auto-ignition temperature which ultimately is the reason for failing to achieve HCCI combustion. Similarly, higher intake air temperature creates higher in-cylinder pressure and temperature which ultimately causes knocking [60, 70].

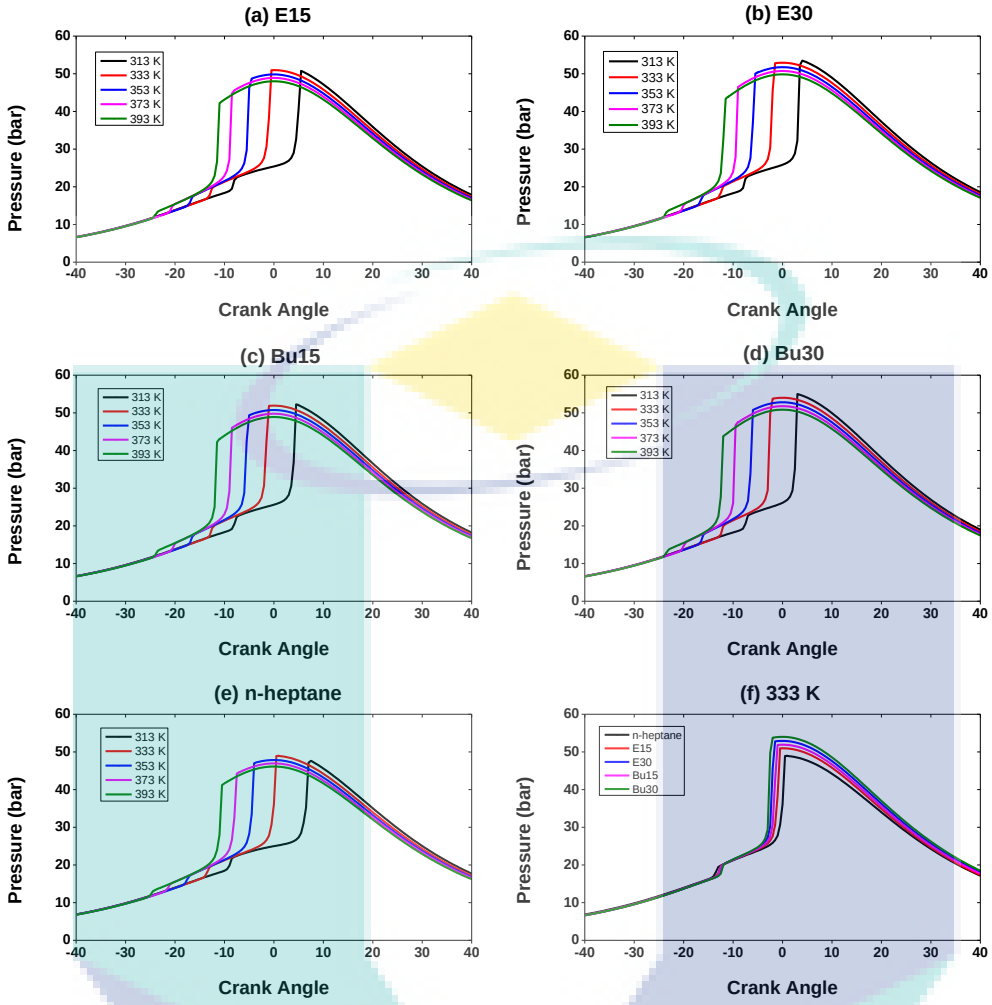

Figure 4.13 The variation of in-cylinder pressure of HCCI combustion at constant lambda λ = 2 and 900 rpm engine speed with different intake temperatures and test fuels

4.4 Combustion Characteristics

The effects of ethanol and butanol fuel blends with n-heptane and neat n-heptane on cylinder pressure and heat release rate dependent on the crank angle with different intake temperatures are presented in Figures 4.13 and 4.14. N-heptane was used as base fuel in the simulations and the test results were compared with n-heptane/ethanol and n-heptane/butanol blends. The pressure rise rate increased a little bit with E30 and Bu30 fuels. It can also be mentioned that SOC was delayed a little bit as the amount of ethanol and butanol increased in the test fuels. Autoignition was increased with the increase of intake temperature for all test fuels. More molecules participated in the chemical reactions. Besides, the chemical reactions were improved between fuel and oxygen molecules at higher intake temperatures [71]. Thus autoignition occurred easily. Maximum cylinder pressure was obtained with E30 and Bu30. Heat release rate increases with the increase of intake temperature up to 15% of ethanol and butanol but it decreases with increasing intake temperature when ethanol and butanol percentage increases up to 30%. It was observed that the most significant effect of intake temperature on HCCI combustion was autoignition timing.

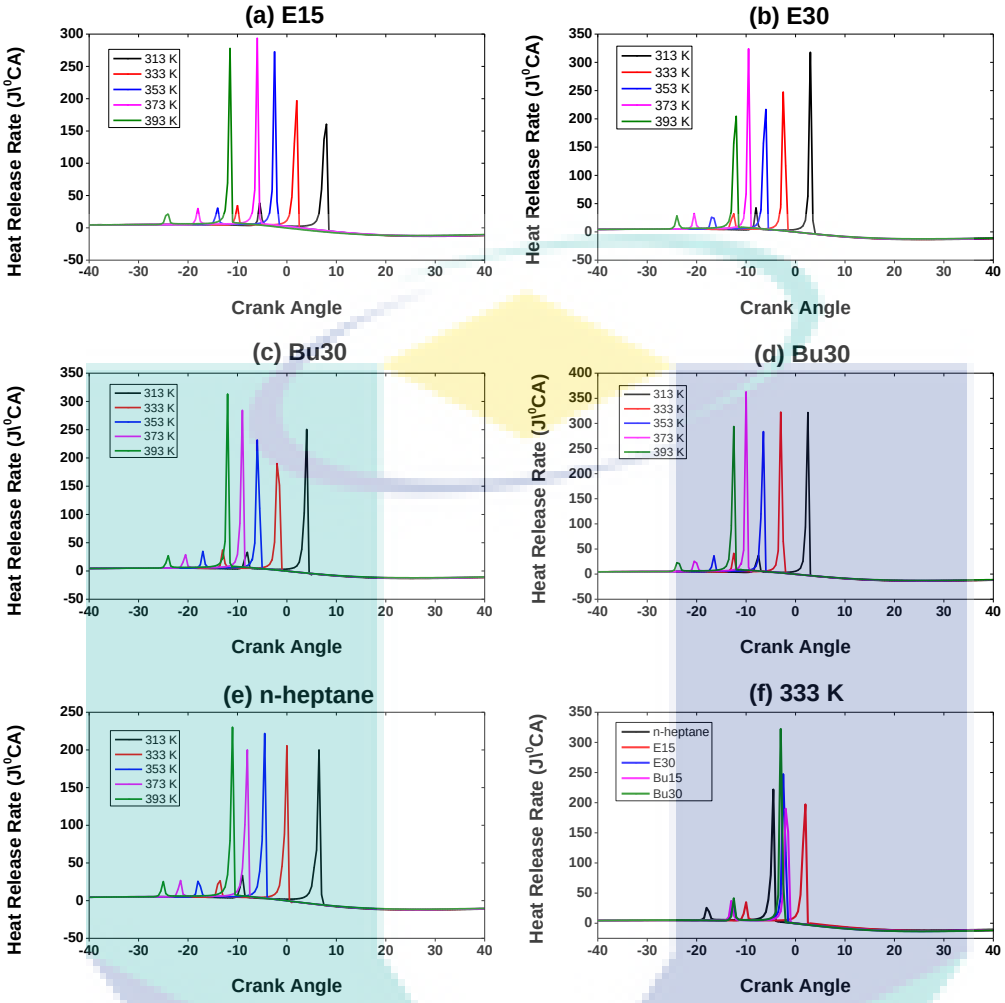

Figure 4.14 The variation of the heat release rate of HCCI combustion at constant lambda, λ = 2 and 900 rpm engine speed with different intake temperatures and test fuels

Although the SOC was affected by the intake temperature, there was a slight difference in cylinder pressure for all test fuels. At high intake temperatures, autoignition can occur easily in HCCI combustion. As can be seen, in Figure 4.14 the start of combustion was delayed with the increase of the amount of the ethanol and butanol in the test fuels. N-heptane was auto-ignited earlier than all the other test fuels due to zero octane number and higher heating value. At 393 K maximum heat release was obtained with Bu15. Maximum cylinder pressure decreased with n-heptane due to earlier autoignition [72]. In-cylinder temperature and pressure should be adequately high at the end of the compression stroke in order to start the chemical reactions in HCCI combustion. The in-cylinder temperature at the end of compression stroke increases with the increase of intake temperature. However, intake temperature is limited because of the higher pressure rise rate on HCCI combustion [68]. It also causes the cyclic variations which are the indication of durability and stability of the internal combustion engines [73].

The effects of intake temperature with different test fuels on SOC are presented in Figure 4.15. SOC is strongly controlled by chemical and physical properties of the fuel, temperature, and pressure at the end of the compression stroke in HCCI combustion [3]. Among them, intake temperature is one of the most

dominant factors affecting the start of autoignition. In this study, SOC was determined with the heat release rate which rises from zero to a positive value. It was found that increased intake temperature caused combustion to advance for each test fuel. Simulation results showed that earliest autoignition was obtained with n-heptane. Minimum SOC was obtained with E30 test fuel. It could be implied that the SOC was delayed as the amount of ethanol and butanol increased in the test fuels because higher octane number alcohol tends to retard the autoignition. Earlier autoignition results in knocking combustion which damages the engine parts [74]. As a result, high octane number alcohol fuel seems to be the most promising alternative fuel in HCCI combustion in order to prevent knocking combustion and to extend operating range.

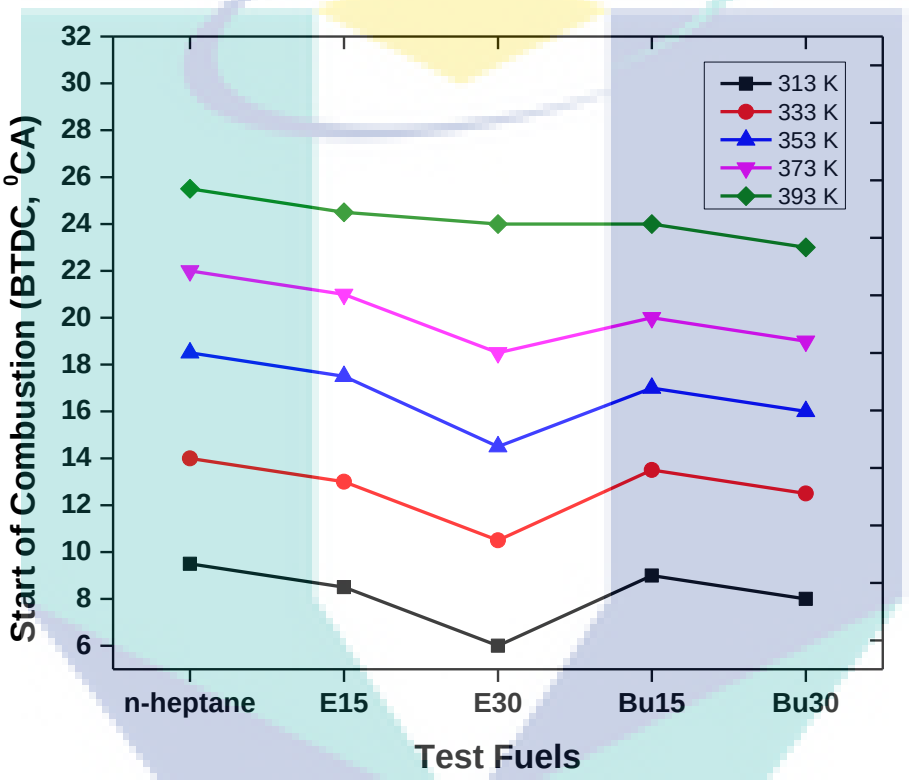

Figure 4.15 The variation of SOC of HCCI combustion at constant lambda, λ = 2 and 900 rpm engine speed with different intake temperatures and test fuels

Figure 4.16 presents the combustion duration (CA50 and CA10–90) of test fuels at different intake temperatures. Figure 4.16 (a) presents the variation of CA50 with test fuels at different intake temperatures. Crank angle degrees define the points versus crank angle where the CA50 was obtained before top dead center. It is seen that CA50 closes to TDC as the intake temperature decreases. CA50 was determined near TDC with Bu30 due to faster combustion. It can be inferred from Figure 4.16(b) that CA10–90 decreases as intake temperature increases. Minimum combustion duration was obtained at 393 K for each test fuel. At high intake temperatures, CA10–90 decreases due to the improvement of chemical reactions and increasing of the activated molecules during the combustion reaction. It results in shorter combustion duration [75]. Furthermore, combustion duration (CA10–90) decreased when the mass fraction of ethanol and butanol increased in the test fuel. It was seen that the increase of octane number of test fuels caused a decrease in combustion duration. The longest combustion duration was obtained with n-heptane due to knocking [72].

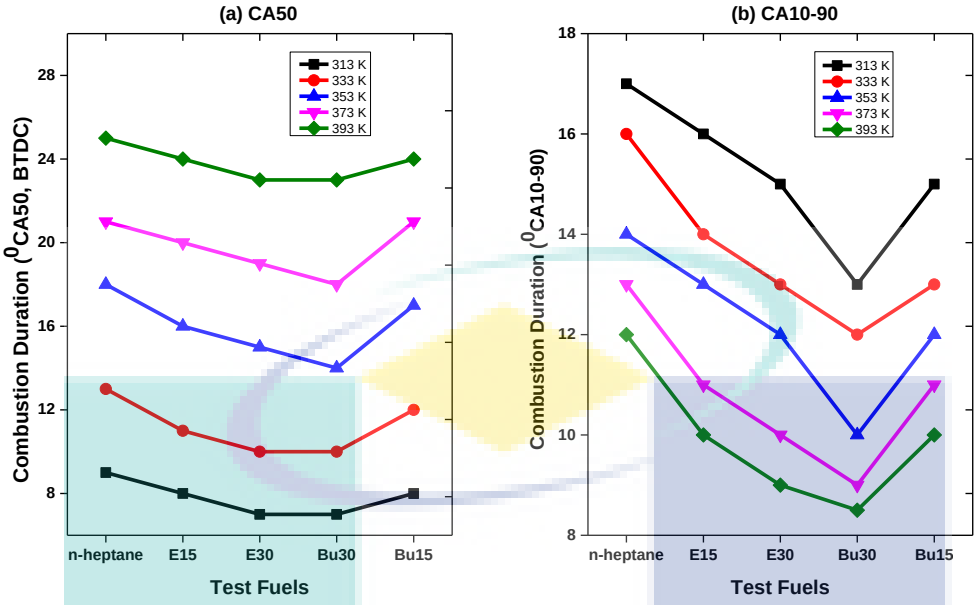

Figure 4.16 The variation of combustion duration (CA50 and CA10-90) of HCCI combustion at constant lambda, λ = 2 and 900 rpm engine speed with different intake temperatures and test fuels

4.5 Performance Characteristics

The variation of IMEP with test fuels at different intake temperatures on HCCI combustion is presented in Figure 4.17. It can be seen that IMEP decreases with the increase of intake temperature. It also causes the decrease of volumetric efficiency at high intake temperatures because hot air has lower density compared to cold air. The simulation has run with the leaner mixture at constant excessive air coefficient λ= 2on HCCI combustion. So, the energy driven to the cylinder decreases. Thus, IMEP decreases especially at high intake temperatures as seen in Figure 4.17. It can be also concluded that IMEP decreases with n-heptane due to knocking although it has higher heating value compared to ethanol and butanol blends. There was no remarkable difference on imep when the E15 was used as a fuel in the simulations. However, IMEP of E30, Bu15 and Bu30 was higher than E15. Maximum imep was obtained with Bu30 as 6.51 bar at 313 K intake temperature. Imep increased by about 13.97% when compared to pure n-heptane at 313 K intake temperature. The reason of imep increase with Bu30 can be explained due to higher calorific value compared to ethanol. In addition, the density of ethanol and butanol is higher than n-heptane. It may be mentioned that it causes to drive more energy into the cylinder compared to n-heptane. Hence, the pressure at the end of combustion increases due to more fuel molecules participation in the chemical reactions [60].

The effects of test fuels and intake temperatures on indicated thermal efficiency (ITE) of HCCI engine are presented in Figure 4.18. Thermal efficiency increased with the increase of intake temperature with n-heptane, E15, Bu15 and Bu30. It can be clearly noticed that autoignition can occur easily at high intake temperatures and autoignition conditions improve at each point of the combustion chamber. Thus, thermal efficiency increases. However, a small decrease was seen in thermal efficiency with n-heptane, E15, and E30 at 393 K intake temperature. It can be said that CA50 was determined a little bit far away from TDC with n-heptane, E15 and E30 compared to other test fuel at 393 K intake temperature because combustion occurred away from TDC. Maximum thermal efficiency was obtained as 54.36% with

Bu30 test fuel at 393 K intake temperature. Similarly, CA50 was determined near TDC with Bu30.

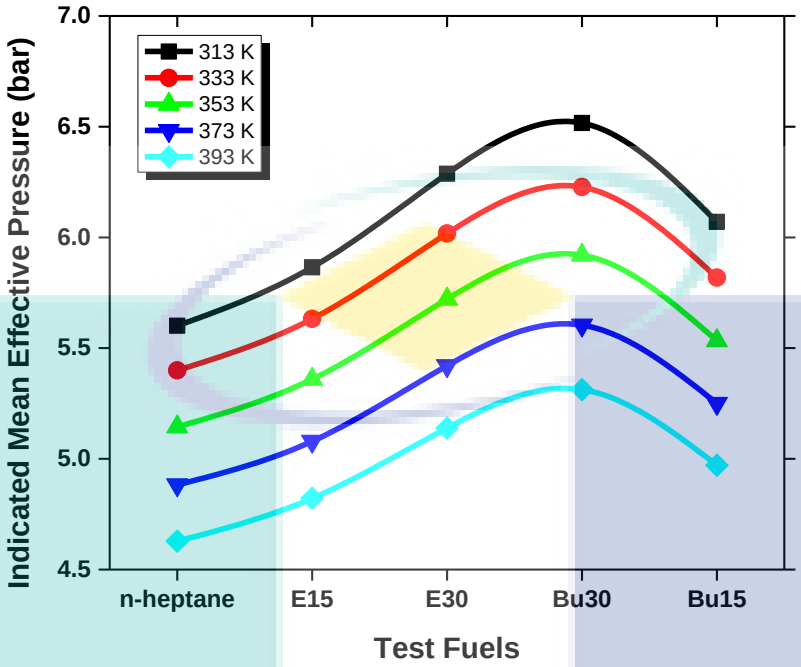

Figure 4.17 The variation of indicated mean effective pressure on HCCI combustion at constant lambda, λ = 2 and 900 rpm engine speed with different intake temperatures and test fuels

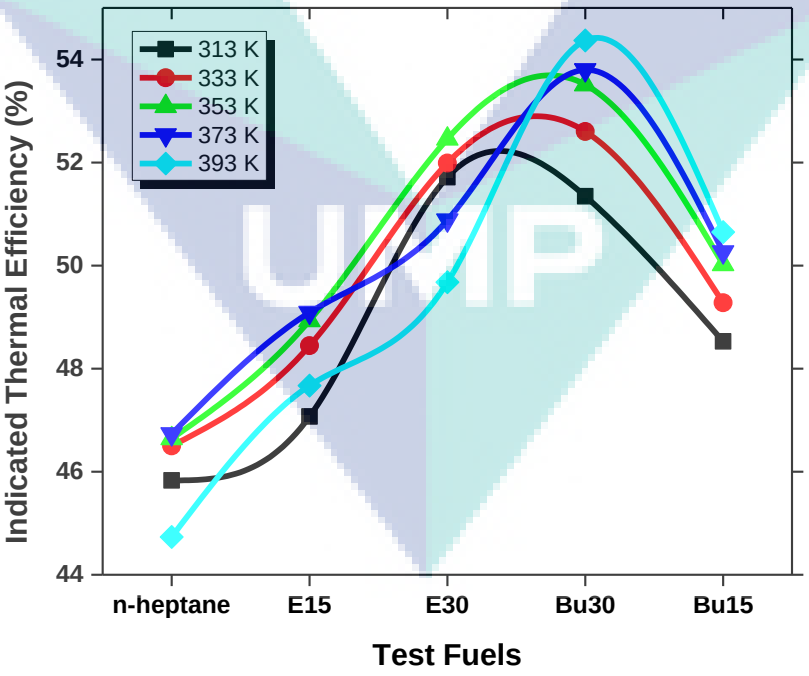

Figure 4.18 The variation of indicated thermal efficiency of HCCI combustion at constant lambda, λ = 2 and 900 rpm engine speed with different intake temperatures and test fuels

Chemical reactions improve when the combustion occurs near TDC due to higher cylinder pressure at smaller volume in the combustion chamber [76]. In

contrast, minimum thermal efficiency was obtained as 45.82% with n-heptane test fuel at 313 K intake temperature. Although combustion occurred close to the top dead center with n-heptane at 313 k intake temperature, knocking tendency was observed with n-heptane test fuel. Thus, thermal efficiency decreased. At 393 K inlet air temperature, thermal efficiency increased by about 17.71% with Bu30 compared to n-heptane. It is also clear that the addition of butanol improves the thermal efficiency compared to ethanol due to the higher heating value of butanol.

4.5.1 Emissions Characteristics

Figure 4.19 presents minimum CO emissions were produced with n-heptane because of higher combustion temperature and faster combustion due to knocking. It can be also concluded that CO emissions decrease with the increase of intake temperature. In the case of lower intake temperature, at the end of combustion, the temperature becomes too low for complete oxidation. Thus CO_2 formation is decreased and the amount of CO emissions increased [72]. Maximum CO emissions were measured at 313 K intake temperature for all test fuels. It is also seen that CO emissions increase with the increase of the amount of ethanol and butanol in the test fuel. The reason behind this phenomenon is that close to the rich limit for HCCI and with early combustion phasing, very little CO is generated. However, close to the lean limit and with late combustion phasing, lot of CO can be formed [74]. The simulations were run with lean mixtures and using ethanol and butanol retarded the SOC. Maximum CO emissions were measured as 0.47% with E30 at 313 K intake temperature. In Figure 4.20, the variation of HC emissions is presented at different intake temperatures using different fuels. HCCI features low temperature combustion, but this low combustion temperature results in higher emissions of hydrocarbons. The combustion temperature near the walls is even lower, due to heat losses.

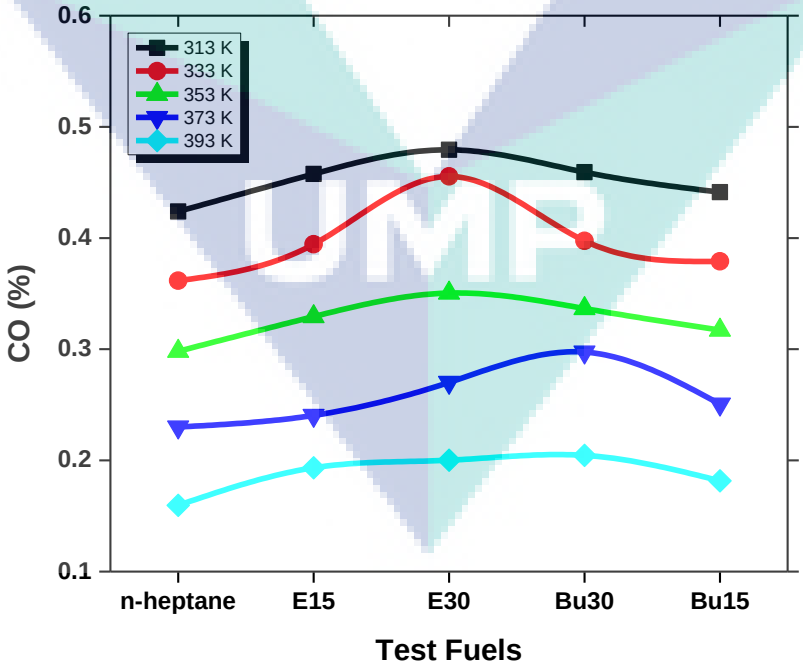

Figure 4.19 The variation of CO emissions on HCCI combustion at constant lambda, λ = 2 and 900 rpm engine speed with different intake temperatures and test fuels.

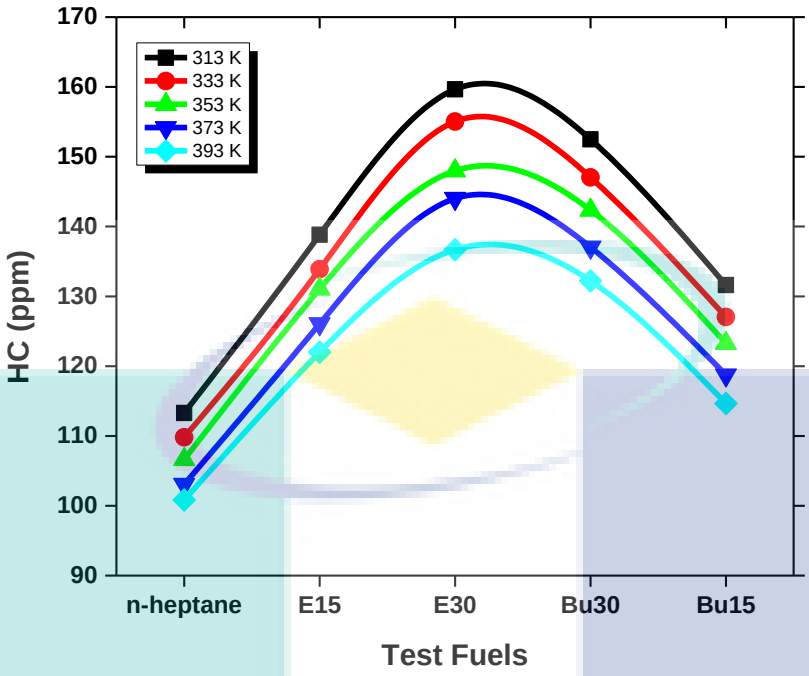

Figure 4.20 The variation of HC emissions on HCCI combustion at constant lambda, λ = 2 and 900 rpm engine speed with different intake temperatures and test fuels

Large parts of the HC emissions originate from the wall regions [77]. Figure 4.20 presents that HC emissions decrease with the increase of intake temperature. The reason for this reduction is that chemical reactions improve and rapid combustion occurs at high intake temperatures. The productions of radicals accelerate with the increase in intake temperature and combustion reactions [78]. Moreover, higher intake temperature decreases the cooling effects of homogeneous leaner charge mixture [12]. It can be mentioned that minimum HC emissions were measured with n-heptane and Bu15 compared to other test fuels. It can be said that autoignition properties are deteriorated and HC emissions are generated when each test fuel is obtained by blending with ethanol and butanol. Maximum HC emissions were measured as 159.664 ppm with E30 test fuel at 313 K intake temperature. The variation of NO_x emissions is presented in Figure 4.21. In the present study, NO_x emissions were found very low which is less than 2.5 ppm with all test fuels at each intake temperature. NO_x emissions can be simultaneously reduced in HCCI combustion because HCCI engines operate with leaner homogenous charge mixtures. NO_x emissions are produced at high combustion temperatures. Thus NO formation mechanisms cannot occur due to the lower end of combustion temperature. This is one of the most important advantages of HCCI combustion. Figure 4.21 presents that NO_x emissions increase with the increase of intake temperature. This is because of the higher in-cylinder temperature with increasing intake temperature. Minimum NO_x emissions were measured with Bu15 and Bu30 test fuel at all intake temperatures.

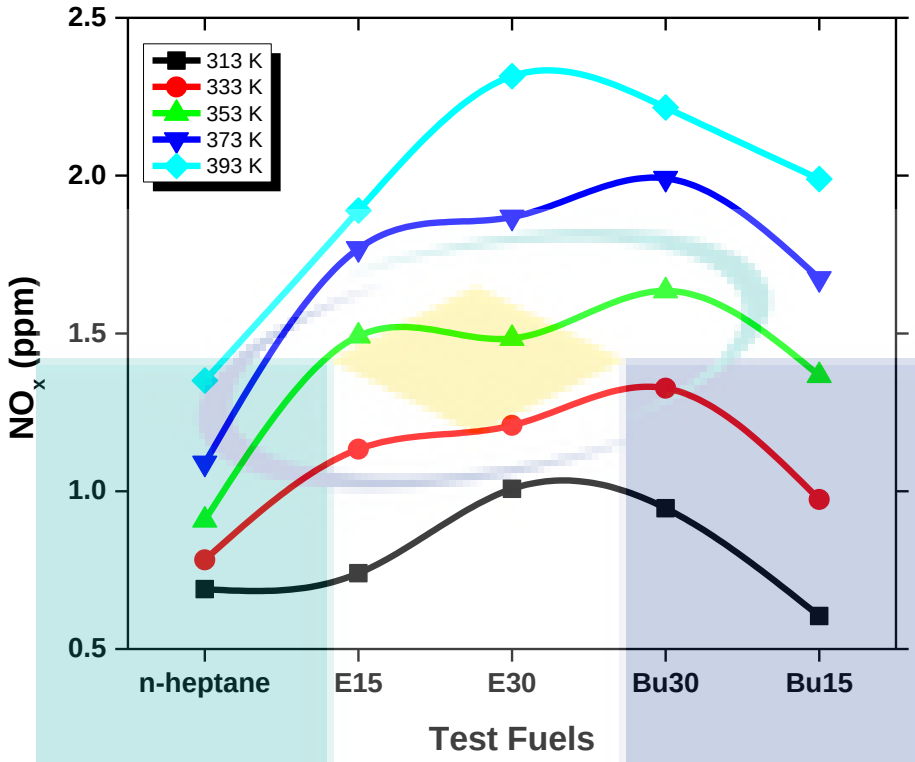

Figure 4.21 The variation of NO_x emissions on HCCI combustion at constant lambda, $\lambda = 2$ and 900 rpm engine speed with different intake temperatures and test fuels

4.6 Summary

The validation results show good agreement with the experimental data and capture important combustion phase trends as engine parameters are varied with a maximum percentage of error which is less than 6% for diesel HCCI and 4% for gasoline HCCI. The effects of different engine parameters on combustion and performance of both diesel and gasoline HCCI engines have also presented. The intake temperature has the most significant effect on HCCI combustion and performance characteristics. The proper controlling of engine parameters can extend the operating range of HCCI engines. This Chapter has also presented the effects of fuel blends on combustion, performance and emissions characteristics of HCCI engines. Both ethanol and butanol has ability to delay the ignition timing which may save HCCI engine from excessive pressure and temperature rise. The engine efficiency and emissions levels can be improved further by utilizing different control parameters such as compression ratio, leaner mixture, exhaust gas recirculation, etc. Therefore, the HCCI engine could be a viable option in the near future.

5. CONCLUSIONS AND RECOMMENDATIONS

A zero dimensional single zone model was established to investigate HCCI combustion, performance and emissions characteristics using pure n-heptane, and ethanol/n-heptane mixtures and butanol/n-heptane mixtures. Various chemical reaction mechanisms were used to solve the chemical reactions during combustion. The validated numerical simulation was able to capture trends in combustion phasing variation with critical engine parameters, particularly the low temperature reaction (LTR). The main combustion stage (MCS) predicted by the numerical simulation is advanced compared to the experimental results because of the assumption of uniform mixture temperature and mixture composition. It was found from the simulation that HCCI combustion was advanced with the increase of intake temperature. When thermal efficiency is examined, butanol has advantage according to ethanol. Thermal efficiency increased by about 17.71% with Bu30 compared to n-heptane at 393 K intake temperature. IMEP decreased at all intake temperatures with n-heptane. Very low amount of NOx emissions were measured with test fuels. NOx emissions were increased with the increase of intake temperature. This is because of the higher in-cylinder temperature with increasing intake temperature. It can be said that CO emissions increased with the increase of alcohol in the test fuels. Higher HC emissions were obtained especially at lower intake temperature when ethanol was used as an additive fuel. It is hoped that this numerical investigation contributes to the determination of proper fuel mixture and intake temperature for the problems such as extending the HCCI operation range, controlling the combustion, and reduction of CO and HC emissions in HCCI combustion.

The main combustion stage (MCS) predicted by the numerical simulation is advanced compared to the experimental data because of the assumption of uniform mixture temperature and mixture composition. It was obtained from the simulation that HCCI combustion was advanced with the increase of inlet air temperature and with the decrease of lambda values. Combustion was also delayed with increasing ethanol addition to test fuels. Because of having lower energy density and higher octane number ethanol prevents the charge to ignite earlier. On the other hand, DEE has a low ignition temperature and higher energy density which helps to achieve HCCI combustion even with lean mixtures. It is possible to say that lower in-cylinder pressure and heat release rate were obtained with increasing lambda values and ethanol amount in the test fuels. Elongated combustion duration was obtained with the increase of inlet air temperature and decrease of lambda values as well as ethanol addition also produced shorter combustion duration. When indicated thermal efficiency and CA50 were examined it was found that with increasing inlet air temperature and decreasing lambda indicated thermal efficiency was increased and CA50 occurred close to TDC. In the case of IMEP, increasing lambda values produced lower IMEP because of lower in-cylinder pressure at the end of combustion for leaner mixtures. The most prominent finding is ethanol addition prevents the charge from earlier combustion which may save the engine from damage by excessive pressure and temperature rise from earlier combustion. It also helps to extend the HCCI operating range.

REFERENCES

[1] Ball M, Wietschel M. The future of hydrogen–opportunities and challenges. International Journal of Hydrogen Energy. 2009;34:615-27.
[2] Celik MB. Experimental determination of suitable ethanol–gasoline blend rate at high compression ratio for gasoline engine. Applied Thermal Engineering. 2008;28:396-404.
[3] Olsson J-O, Tunestål P, Johansson B, Fiveland S, Agama JR, Assanis DN. Compression ratio influence on maximum load of a natural gas fueled HCCI engine. SAE Transactions, Journal of Engines. 2002;111:442-58.
[4] Zhen X, Wang Y, Xu S, Zhu Y, Tao C, Xu T, et al. The engine knock analysis–An overview. Applied Energy. 2012;92:628-36.
[5] Hasan M, Rahman M. Homogeneous charge compression ignition combustion: Advantages over compression ignition combustion, challenges and solutions. Renewable and Sustainable Energy Reviews. 2016;57:282-91.
[6] Raitanapaibule K, Aung K. Performance predictions of a hydrogen-enhanced natural gas HCCI engine. ASME 2005 International Mechanical Engineering Congress and Exposition: American Society of Mechanical Engineers; 2005. p. 289-94.
[7] Epping K, Aceves S, Bechtold R, Dec JE. The potential of HCCI combustion for high efficiency and low emissions. SAE Technical Paper; 2002.
[8] Kong S-C, Reitz RD. Use of detailed chemical kinetics to study HCCI engine combustion with consideration of turbulent mixing effects. Journal of engineering for gas turbines and power. 2002;124:702-7.
[9] Najt PM, Foster DE. Compression-ignited homogeneous charge combustion. SAE Technical paper; 1983.
[10] Zhao H. HCCI and CAI Engines for the Automotive Industry: Elsevier; 2007.
[11] Ericson C, Andersson M, Egnell R, Westerberg B. Modelling diesel engine combustion and NOx formation for model based control and simulation of engine and exhaust aftertreatment systems. SAE paper. 2006:0687.
[12] Gan S, Ng HK, Pang KM. Homogeneous charge compression ignition (HCCI) combustion: implementation and effects on pollutants in direct injection diesel engines. Applied Energy. 2011;88:559-67.
[13] Miller JA, Bowman CT. Mechanism and modeling of nitrogen chemistry in combustion. Progress in energy and combustion science. 1989;15:287-338.
[14] Ishii H, Koike N, Suzuki H, Odaka M. Exhaust purification of diesel engines by homogeneous charge with compression ignition Part 2: Analysis of combustion phenomena and NOx formation by numerical simulation with experiment. SAE Technical Paper; 1997.
[15] Tree DR, Svensson KI. Soot processes in compression ignition engines. Progress in Energy and Combustion Science. 2007;33:272-309.
[16] Soloiu V, Duggan M, Ochieng H, Williams D, Molina G, Vlcek B. Investigation of Low Temperature Combustion Regimes of Biodiesel With n-Butanol Injected in the Intake Manifold of a Compression Ignition Engine. Journal of Energy Resources Technology. 2013;135:041101.
[17] Izadi Najafabadi M, Abdul Aziz N. Homogeneous charge compression ignition combustion: challenges and proposed solutions. Journal of combustion. 2013;2013.
[18] Yao M, Zheng Z, Liu H. Progress and recent trends in homogeneous charge compression ignition (HCCI) engines. Progress in Energy and Combustion Science. 2009;35:398-437.
[19] Saxena S, Bedoya ID. Fundamental phenomena affecting low temperature combustion and HCCI engines, high load limits and strategies for extending these limits. Progress in Energy and Combustion Science. 2013;39:457-88.

[20] Mangus M, Kiani F, Mattson J, Depcik C, Peltier E, Stagg-Williams S. Comparison of neat biodiesels and ULSD in an optimized single-cylinder diesel engine with electronically-controlled fuel injection. Energy & Fuels. 2014;28:3849-62.
[21] Komninos N, Rakopoulos C. Modeling HCCI combustion of biofuels: A review. Renewable and Sustainable Energy Reviews. 2012;16:1588-610.
[22] Pei Y, Mehl M, Liu W, Lu T, Pitz WJ, Som S. A Multicomponent Blend as a Diesel Fuel Surrogate for Compression Ignition Engine Applications. Journal of Engineering for Gas Turbines and Power. 2015;137:111502.
[23] Sarathy SM, Westbrook CK, Mehl M, Pitz WJ, Togbe C, Dagaut P, et al. Comprehensive chemical kinetic modeling of the oxidation of 2-methylalkanes from C 7 to C 20. Combustion and flame. 2011;158:2338-57.
[24] Lu T, Plomer M, Luo Z, Sarathy S, Pitz W, Som S, et al. Directed relation graph with expert knowledge for skeletal mechanism reduction. 7th US national combustion meeting, Atlanta, GA2011.
[25] Mehl M, Chen J-Y, Pitz WJ, Sarathy S, Westbrook CK. An approach for formulating surrogates for gasoline with application toward a reduced surrogate mechanism for CFD engine modeling. Energy & Fuels. 2011;25:5215-23.
[26] Mehl M, Pitz WJ, Westbrook CK, Curran HJ. Kinetic modeling of gasoline surrogate components and mixtures under engine conditions. Proceedings of the Combustion Institute. 2011;33:193-200.
[27] Mehl M, Pitz W, Sarathy M, Yang Y, Dec JE. Detailed kinetic modeling of conventional gasoline at highly boosted conditions and the associated intermediate temperature heat release. SAE Technical Paper; 2012.
[28] Dec JE, Yang Y. Boosted HCCI for high power without engine knock and with ultra-low NOx emissions-using conventional gasoline. SAE International Journal of Engines. 2010;3:750-67.
[29] Seiser R, Pitsch H, Seshadri K, Pitz W, Gurran H. Extinction and autoignition of n-heptane in counterflow configuration. Proceedings of the Combustion Institute. 2000;28:2029-37.
[30] Dagaut P, Togbé C. Experimental and modeling study of the kinetics of oxidation of ethanol-n-heptane mixtures in a jet-stirred reactor. Fuel. 2010;89:280-6.
[31] Dagaut P, Togbé C. Experimental and modeling study of the kinetics of oxidation of butanol− n-heptane mixtures in a jet-stirred reactor. Energy & Fuels. 2009;23:3527-35.
[32] Golub A, Ghoniem A. Modeling NOx formation in a small bore, lean natural gas, spark ignition engine. SAE Technical Paper; 1999.
[33] Amnéus P, Mauss F, Kraft M, Vressner A, Johansson B. NOx and N2O formation in HCCI engines. SAE Technical Paper; 2005.
[34] Miller JA, Pilling MJ, Troe J. Unravelling combustion mechanisms through a quantitative understanding of elementary reactions. Proceedings of the Combustion Institute. 2005;30:43-88.
[35] Mueller MA, Yetter RA, Dryer FL. Kinetic modeling of the CO/H2O/O2/NO/SO2 system: Implications for high-pressure fall-off in the SO2 + O(+M) = SO3(+M) reaction. International Journal of Chemical Kinetics. 2000;32:317-39.
[36] Heywood JB. Internal combustion engine fundamentals: Mcgraw-hill New York; 1988.
[37] Assanis D, Polishak M. Valve event optimization in a spark-ignition engine. Journal of Engineering for Gas Turbines and Power. 1990;112:341-7.
[38] Stiesch G. Modeling engine spray and combustion processes: Springer Science & Business Media; 2013.
[39] Kuo KK. Principles of combustion. 1986.

[40] Assanis DN, Heywood JB. Development and use of a computer simulation of the turbocompounded diesel system for engine performance and component heat transfer studies. SAE Technical Paper; 1986.
[41] Shaver GM, Gerdes JC, Jain P, Caton P, Edwards C. Modeling for control of HCCI engines. American Control Conference, 2003 Proceedings of the 2003: IEEE; 2003. p. 749-54.
[42] Canova M, Garcin R, Midlam-Mohler S, Guezennec Y, Rizzoni G. A control-oriented model of combustion process in a HCCI diesel engine. American Control Conference, 2005 Proceedings of the 2005: IEEE; 2005. p. 4446-51.
[43] Killingsworth NJ, Aceves SM, Flowers DL, Krstić M. A simple HCCI engine model for control. Computer Aided Control System Design, 2006 IEEE International Conference on Control Applications, 2006 IEEE International Symposium on Intelligent Control, 2006 IEEE: IEEE; 2006. p. 2424-9.
[44] Guo H, Neill WS, Chippior W, Li H, Taylor JD. An experimental and modeling study of HCCI combustion using n-heptane. Journal of Engineering for Gas Turbines and Power. 2010;132:022801.
[45] Gotoh S, Kuboyama T, Moriyoshi Y, Hatamura K, Yamada T, Takanashi J, et al. Evaluation of the Performance of a Boosted HCCI Gasoline Engine with Blowdown Supercharge System. SAE Technical Paper; 2013.
[46] Andrae J. A kinetic modeling study of self-ignition of low alkylbenzenes at engine-relevant conditions. Fuel Processing Technology. 2011;92:2030-40.
[47] Bunting BG, Eaton S, Naik CV, Puduppakkam KV, Chou C-P, Meeks E. A Comparison of HCCI Ignition Characteristics of Gasoline Fuels Using a Single-Zone Kinetic Model with a Five Component Surrogate Fuel. SAE Technical Paper; 2008.
[48] Zheng QP, Zhang HM. A computational study of combustion in compression ignition natural gas engine with separated chamber. Fuel. 2005;84:1515-23.
[49] Soyhan H, Yasar H, Walmsley H, Head B, Kalghatgi G, Sorusbay C. Evaluation of heat transfer correlations for HCCI engine modeling. Applied Thermal Engineering. 2009;29:541-9.
[50] Wang Z, Shuai S-J, Wang J-X, Tian G-H, An X-L. Modeling of HCCI combustion: From 0D to 3D. SAE Technical Paper; 2006.
[51] Barroso G, Escher A, Boulouchos K. Experimental and numerical investigations on HCCI-combustion. 7th International Conference on Engines for Automobile: Citeseer; 2005.
[52] Zhou P, Zhou S, Clelland D. A modified quasi-dimensional multi-zone combustion model for direct injection diesels. International Journal of Engine Research. 2006;7:335-45.
[53] An H, Yang W, Chou S, Chua K. Combustion and emissions characteristics of diesel engine fueled by biodiesel at partial load conditions. Applied Energy. 2012;99:363-71.
[54] Su H, Mosbach S, Kraft M, Bhave A, Kook S, Bae C. Two-stage fuel direct injection in a diesel fuelled HCCI engine. SAE paper. 2007:01-1880.
[55] Zhang C, Wu H. Combustion characteristics and performance of a methanol fueled homogenous charge compression ignition (HCCI) engine. Journal of the Energy Institute. 2015.
[56] García MT, Aguilar FJJ-E, Lencero TS. Experimental study of the performances of a modified diesel engine operating in homogeneous charge compression ignition (HCCI) combustion mode versus the original diesel combustion mode. Energy. 2009;34:159-71.
[57] Zhang CH, Xue L, Wang J. Experimental study of the influence of λ and intake temperature on combustion characteristics in an HCCI engine fueled with n-heptane. Journal of the Energy Institute. 2014;87:175-82.

[58] Canakci M. An experimental study for the effects of boost pressure on the performance and exhaust emissions of a DI-HCCI gasoline engine. Fuel. 2008;87:1503-14.
[59] Nishi M, Kanehara M, Iida N. Assessment for innovative combustion on HCCI engine by controlling EGR ratio and engine speed. Applied Thermal Engineering. 2016;99:42-60.
[60] Uyumaz A. An experimental investigation into combustion and performance characteristics of an HCCI gasoline engine fueled with n-heptane, isopropanol and n-butanol fuel blends at different inlet air temperatures. Energy Conversion and Management. 2015;98:199-207.
[61] Peng Z, Zhao H, Ma T, Ladommatos N. Characteristics of homogeneous charge compression ignition (HCCI) combustion and emissions of n-heptane. Combustion science and technology. 2005;177:2113-50.
[62] Liu H, Yao M, Zhang B, Zheng Z. Effects of inlet pressure and octane numbers on combustion and emissions of a homogeneous charge compression ignition (HCCI) engine. Energy & Fuels. 2008;22:2207-15.
[63] Christensen M, Johansson B. Supercharged homogeneous charge compression ignition (HCCI) with exhaust gas recirculation and pilot fuel. SAE Technical Paper; 2000.
[64] Olsson J-O, Tunestål P, Johansson B. Boosting for high load HCCI. SAE Technical Paper; 2004.
[65] Hosseini V, Checkel MD. Intake pressure effects on HCCI combustion in a CFR engine. Proceedings of the combustion institute, canadian section, spring technical meeting2007.
[66] Olsson J-O, Tunestål P, Haraldsson G, Johansson B. A turbocharged dual-fuel HCCI engine. SAE Special Publications. 2001;2001.
[67] Li H, Guo H, Neill WS, Chippior W, Taylor JD. An experimental and modeling study of HCCl combustion using n-heptane. Proceedings of the ICEF2006. 2006:1-11.
[68] Dec JE. Advanced compression-ignition engines—understanding the in-cylinder processes. Proceedings of the combustion institute. 2009;32:2727-42.
[69] Padala S, Woo C, Kook S, Hawkes ER. Ethanol utilisation in a diesel engine using dual-fuelling technology. Fuel. 2013;109:597-607.
[70] Cinar C, Uyumaz A, Solmaz H, Sahin F, Polat S, Yilmaz E. Effects of intake air temperature on combustion, performance and emission characteristics of a HCCI engine fueled with the blends of 20% n-heptane and 80% isooctane fuels. Fuel Processing Technology. 2015;130:275-81.
[71] Ra Y, Reitz RD. A reduced chemical kinetic model for IC engine combustion simulations with primary reference fuels. Combustion and Flame. 2008;155:713-38.
[72] Lü X, Hou Y, Zu L, Huang Z. Experimental study on the auto-ignition and combustion characteristics in the homogeneous charge compression ignition (HCCI) combustion operation with ethanol/n-heptane blend fuels by port injection. Fuel. 2006;85:2622-31.
[73] Agarwal AK. Biofuels (alcohols and biodiesel) applications as fuels for internal combustion engines. Progress in Energy and Combustion Science. 2007;33:233-71.
[74] Maurya RK, Agarwal AK. Experimental study of combustion and emission characteristics of ethanol fuelled port injected homogeneous charge compression ignition (HCCI) combustion engine. Applied Energy. 2011;88:1169-80.
[75] Lu X, Ji L, Ma J, Zhou X, Huang Z. Combustion characteristics and influential factors of isooctane active-thermal atmosphere combustion assisted by two-stage reaction of n-heptane. Combustion and Flame. 2011;158:203-16.
[76] Yu C, Bari S, Ameen A. A comparison of combustion characteristics of waste cooking oil with diesel as fuel in a direct injection diesel engine. Proceedings of the Institution of Mechanical Engineers, Part D: Journal of Automobile Engineering. 2002;216:237-43.

[77] Christensen M, Johansson B. Homogeneous charge compression ignition with water injection. SAE Special Publications. 1999;1999.
[78] Abd-Alla G, Soliman H, Badr O, Abd-Rabbo M. Effects of diluent admissions and intake air temperature in exhaust gas recirculation on the emissions of an indirect injection dual fuel engine. Energy Conversion and Management. 2001;42:1033-45.